Alma Mater Studiorum - Università di Bologna

DOTTORATO DI RICERCA IN

SCIENZE CARDIO NEFRO TORACICHE

Ciclo 35

Settore Concorsuale: 06/E1 - CHIRURGIA CARDIO - TORACO - VASCOLARE

Settore Scientifico Disciplinare: MED/21 - CHIRURGIA TORACICA

IDENTIFICATION OF MOLECULAR BIOMARKERS IN ESOPHAGEAL ADENOCARCINOMA

Presentata da: Arianna Orsini

Coordinatore Dottorato

Gaetano Domenico Gargiulo

Supervisore

Elena Bonora

Esame finale anno 2023

Abstract

Esophageal adenocarcinoma (EAC) is a severe cancer that has been on the rise in Western nations over the past few decades. It has a high mortality rate because prognosis is generally dismal and the 5-year survival rate is only 35%–45%. Although numerous studies at the genetic level have included EAC in a group of tumors with one of the highest rates of copy number alterations (CNAs), somatic structural rearrangements, high mutation frequency, with different mutational signatures, and with epigenetic mechanisms, the pathogenesis of EAC is still poorly understood. The vast heterogeneity of EAC mutations makes it challenging to comprehend the biology that underlies tumor onset and development, identify prognostic biomarkers, and define a molecular classification to stratify patients. This ultimately hinders the development of targeted therapeutic options for better personalized care. The only way to resolve the current disagreements is through an exhaustive molecular analysis of EAC.

Due to these factors, we examined the genetic profile of 164 patients' esophageal adenocarcinoma samples (without chemo-radiotherapy). The included patients did not receive neoadjuvant therapies, which can change the genetic and molecular composition of the tumor. Using next-generation sequencing technologies (NGS) at high coverage, we examined a custom panel of 26 cancer-related genes.

Over the entire cohort, 337 variants were found, with the *TP53* gene showing the most frequent alteration (67.27%). Poorer cancer-specific survival was associated with missense mutations in the *TP53* gene (Log Rank P=0.0197). We discovered *HNF1alpha* gene disruptive mutations in 7 cases that were also affected by other gene changes. We started to investigate its role in EAC cell lines by silencing HNF1alpha to mimic our EAC cohort and we use Seahorse technique to analyze its role in the metabolism in esophageal cell. No significant changes were found in transfected cell lines.

We conclude by finding that a particular class of TP53 mutations (missense changes) adversely impacted cancer-specific survival in EAC. HNF1alpha, a new EAC-mutated gene, was found, but more research is required to fully understand its function as a tumor suppressor gene.

Introduction

Esophageal adenocarcinoma

Esophageal cancer (EC) is the eighth most common cancer in the world [1]. It is characterized by a poor prognosis, high mortality, and variability in geographical location.

It is a deadly aggressive malignancy with an average 5-year survival rate of 18.4%, indicating the need to identify more effective treatments [2]. This is the sixth most prevalent cause of death and the eighth most common type of cancer globally. With a peak incidence in the sixth to seventh decade, esophageal cancer is an older age-related disease [3].

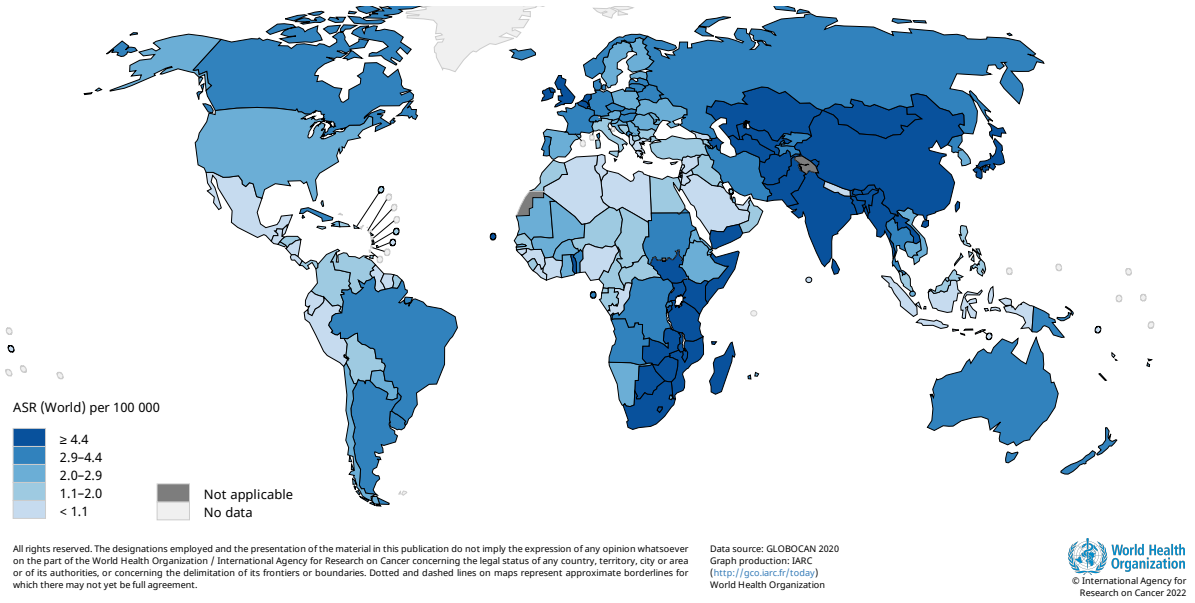

Figure 1. Estimated age-standardized incidence in world (2020) of esophageal cancer. *(From World Health Organization)*

The specific cause(s) of esophageal cancer is unclear; indeed, EC occurs when cells in the esophagus develop changes (mutations) in their DNA causing cells grow and divide out of control. The accumulating abnormal cells form a tumor in the esophagus that can grow to invade nearby structures and spread to other parts of the body.

Esophageal cancer is classified according to the type of cells that are involved which may help to determine treatment options. Esophageal adenocarcinoma (EAC) and Esophageal Squamous Cell Carcinoma (ESCC) are the most common types of EC. There are also some rare forms of esophageal cancer as small cell carcinoma, sarcoma, lymphoma, melanoma and choriocarcinoma.

ESCC is the most prevalent esophageal cancer worldwide, especially in East Asia [3]. It is linked to smoking and tobacco use and occurs most often in the upper and middle portions of the esophagus in the thin, flat cells lining the inside of the esophagus, and the precursor lesion is squamous dysplasia. EAC, instead is the most common form of esophageal cancer in the Western countries, and it affects primarily white men [4]. It is associated with obesity and gastroesophageal reflux disease (GERD), and is originated in the lower part of the esophagus from the glandular cells which produce and release fluids such as mucus.

The causes of the current lethality of EAC may be mostly related to the insufficiency of screening, early diagnosis programs, the relative inefficiency of diagnosis and therapies. Despite the adoption of intensive therapeutic protocols involving surgery, chemotherapy, and radiotherapy, the success of not modulated therapy may be hampered by diverse biological characteristics, according to recent study, which suggests that EAC may be consistently heterogeneous [5].

EAC was found in a group of tumors with one of the highest rates of copy number alterations (CNAs) and somatic structural rearrangements in several genomic investigations. Cell cycle abnormalities, aneuploidy, and mutational inactivation of the p16 and p53 genes are a few examples of the genetic abnormalities that may gradually accumulate to cause EAC [6] as showed in Figure 2. A single genetic occurrence cannot fully explain the complex molecular mechanism [7].

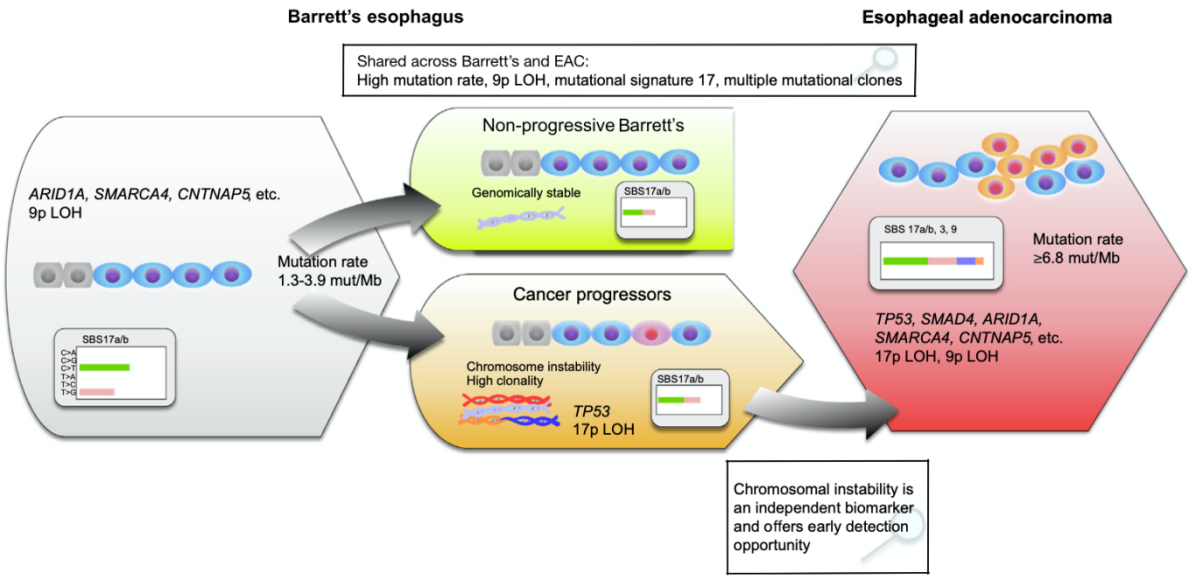

Figure 2: Barrett's esophagus and esophageal adenocarcinoma (EAC) mutational events. *(From Killcoyne et al. 2021)*

Copy number changes (amplifications and deletions) are frequent; amplifications with potential therapeutic value are frequently found receptor tyrosine kinases involved in cell signalling (ERBB2, EGFR, KRAS, FGFR2), in cell cycle regulators (CCND1, CDK6) and in transcription factors (MYC, GATA4, GATA6) [8], [9]. Drug development is complicated by the fact that co-amplification of receptor tyrosine kinases, such as ERBB2 and EGFR, is common in EAC and is likely linked to both de novo and acquired resistance to targeted therapy [10]. Chromosomal instability numerical (CIN) is associated with EAC and is the most common form of structural variation in the cancer genome providing significant genomic diversity in the cancer genome. Targeted therapies are difficult to develop because of the heterogeneity and co-amplification profiles of EAC; however, other methods of locating molecular subgroups may offer opportunities for therapeutic intervention.

Pathogenesis and risk factors

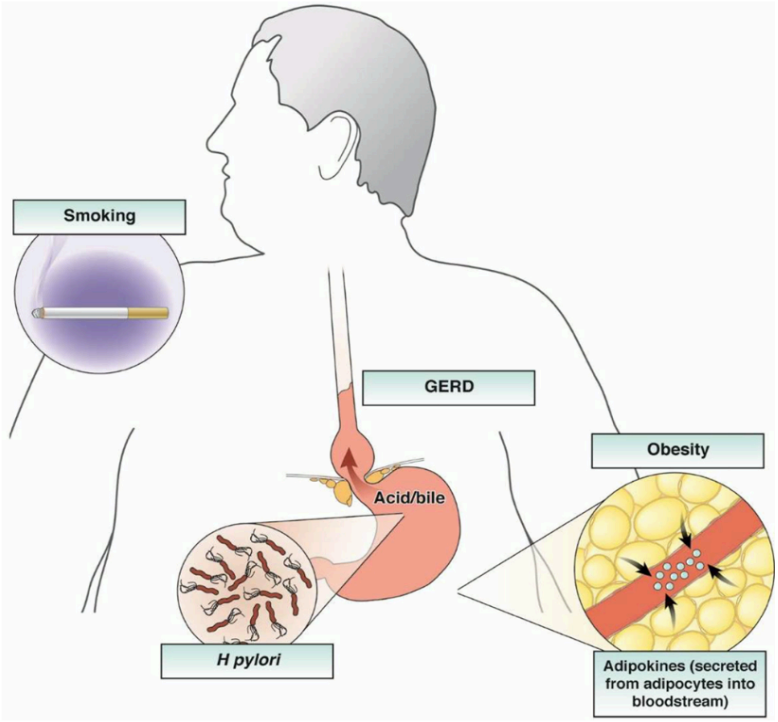

Figure 3. Risk factors of esophageal adenocarcinoma. *(From Rubenstein et al. 2016)*

Gastroesophageal reflux disease (GERD)

In predisposed individuals, GERD is thought to cause erosive esophagitis and, following an abnormal healing process, a metaplastic, specialized intestinal epithelium Barrett's esophagus (BE) [11]. According to a meta-analysis of population-based studies, weekly GERD

symptoms increase the risk of EAC by about 5-fold [12]. Patients with long-standing symptoms, nocturnal symptoms, or symptoms that occur more frequently are at greater risk. The severity of the symptoms, however, is not associated with an increased risk of EAC. Although GERD is an important risk factor for EAC, most individuals with GERD never develop EAC. A systematic review of population-based studies discovered that a slight majority of patients with EAC deny any significant prior GERD symptoms [13].

Tobacco and alcohol use

Data analysis from a group of researchers found a 2.18-fold (95% CI, 1.84-2.58) increase in the risk of EAC associated with tobacco use [14]. Alcohol consumption has not been proven to be a reliable risk factor for EAC, despite being a significant risk factor for esophageal squamous cell carcinoma. In actuality, drinking alcohol and the risk of EAC seem to be moderately inversely related. It is unclear whether drinking alcohol helps prevent EAC; it is also possible that those who develop EAC avoid drinking because it makes their GERD symptoms worse [15].

Obesity

EAC has obesity as a risk factor. In comparison to a BMI of less than 25 kg/m2, a body mass index (BMI) of 30–34.9 kg/m2 is associated with a 2.39-fold increase in risk EAC, with stronger associations for those with even higher BMIs. BE and EAC are both associated with abdominal obesity in particular [16]. Hiatal hernia is mechanically encouraged by obesity and is associated with a higher risk of GERD [17] [18]. In addition to its mechanical effects, abdominal obesity is linked to alterations in the blood levels of peptides linked to Barrett's esophagus, which may also promote EAC [19]. Abdominal obesity is associated with insulin resistance and hyperinsulinemia, which have been linked to numerous epithelial malignancies [20]. The metabolic syndrome has been connected to EAC and BE. Evidence linking diabetes mellitus or hyperinsulinemia to BE or EAC, however, has been ambiguous [19] [21], [22]. The development of EAC has been associated with the insulin-like growth factor (IGF) pathway more so than with insulin itself. The presence of Barrett's esophagus is inversely correlated with blood levels of IGF binding protein-3 [23]. A variation in the IGF1 receptor gene alters how obesity affects the likelihood of developing BE and EAC, and a polymorphism in the IGF1 gene is linked to Barrett's esophagus [24]. Participation of the IGF pathway may also increase the likelihood of EAC developing from BE [25].

Helicobacter pylori (H. pylori) infection

It appears that *H. pylori* infection provides EAC defense, in fact people with EAC have a nearly 50% lower risk of developing *H. pylori* infection than those without it [26]. The *H. pylori* strain with the cytotoxin-associated gene A appears to reduce the prevalence of EAC, as a matter of fact infection that primarily affects the gastric body, or the body and the antrum, lowers the risk of acidic GERD and EAC [27]; but an antrum-focused illness may also be accompanied by a rise in gastrin, which in turn raises stomach acid production. Given that the majority of *H. pylori* infections in Western countries occur mostly in the antrum, it is unclear whether the inverse relationship between *H. pylori* and EAC is brought on by a lower prevalence of GERD. In Western nations, the relationship between *H pylori* infection and GERD does not seem to be as strong as it is in Asian nations [28]. Refluxed *H. pylori* DNA may also lessen the inflammatory response to GERD, which is another way that *H. pylori* infection lowers the risk of EAC [29]. People with a genetic predisposition for *H. pylori* infection may also have a propensity for an inflammatory response to GERD [30]. The lack of *H. pylori* infection may only serve as a marker for other modifications to the esophageal and/or stomach microbiome that are directly linked to the onset of EAC [31]. The mechanisms underlying the association between *H. pylori* and EAC require further study.

Barrett's Esophagus

Esophageal adenocarcinoma develops from a pre-neoplastic precursor Barrett's esophagus (BE), which is characterized by the replacement of stratified squamous epithelium in the distal esophagus with specialized or intestinal-like columnar epithelium (Figure 4).

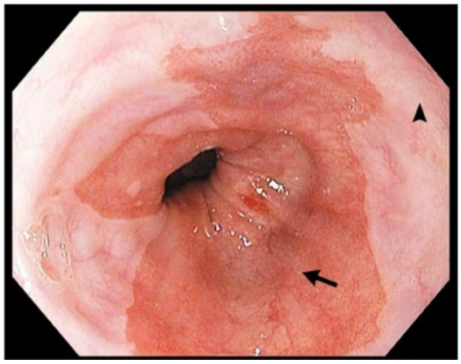

Figure 4: Representation of esophagus with alteration known as Barrett's esophagus (arrow). *(From Curtius et al. 2020)*

BE is formed in response to reflux injury to the lower esophagus caused by chronic gastroesophageal reflux disease (GERD) and esophageal inflammation [8]. In the general population, the baseline risk for EAC is low, but it is 30-125 times higher in patients with BE [32] [33]; the yearly risk for EAC in non-dysplastic BE is approximately 0.27-0.5% per person-year [34]. Once developed, EAC has a poor prognosis, with a 5-year survival rate of less than 15% [35]. As a result, it is critical to understand the molecular mechanisms of BE.

Patients with BE are currently advised to undergo routine endoscopic surveillance, during which biopsies are examined for histopathologic signs of progression, particularly dysplasia [36]. Because short segment BE initial biopsy evaluation can miss metaplasia, the quantity of biopsy samples is crucial. However, using dysplasia as the sole sign of increased cancer risk has some drawbacks. First, there is a significant inter-observer variation in the histologic grading of dysplasia [33][34]. Second, despite the large number of patients with non-dysplastic BE, there are no established biomarkers that can be used to determine who is at risk (NDBE). The current patient-finding strategies for surveillance that search for patients in the period of time between the onset of dysplasia and the onset of advanced cancer may be ineffective, as proof now proposes that the transformation from dysplasia to cancer can occur faster than previously suspected [39]. Improved techniques to identify high-risk patients with BE just before onset of dysplasia both might increase the effectiveness of screening and provide economic value by focusing assets on the small fraction of BE patients who could eventually progress. In an effort to enhance patient stratification, previous biomarker studies have looked at mutations, chromosomal changes, copy number/aneuploidy [40], and gene methylation [40], [41]. Barrett's mucosa, a pre-neoplastic tissue where columnar intestinal type mucosa replaces squamous esophageal epithelium, frequently has somatic genetic alterations that make it more likely to develop cancer. *TP53* and *SMAD4* are two of the few mutated genes that appear to occur in a stage-specific manner, which may be useful for identifying patients who are at risk of developing EAC [42]. Loss of heterozygosity of several loci, particularly 17p and 9p, which contain the tumor suppressor genes *TP53* and *CDKN2A*, is another genetic abnormality that is frequent in BE [43]. The tumor suppressor p53 has been identified as a potential risk factor for BE progression through mutation or aberrant expression [44]. However, p53 IHC is not currently recommended for risk stratification [45].

An optimized approach to determine which patients are at increased risk of progression, especially among the large population of those with non-dysplastic BE, would greatly aid in the development of more effective surveillance and treatment strategies.

Diagnosis and treatments

The majority of EAC patients show up with advanced disease and symptoms. Only about 25% of EAC patients have localized disease at the time of presentation [46] which severely restricts the availability of efficient treatments.

Endoscopic procedure: endoscopic submucosal dissection (ESD) and endoscopic mucosal resection (EMR) both provide the depth of invasion, which is the most crucial piece of prognostic data from endoscopic resection and allows the tumor to be staged. EAC can show up during an endoscopy as a stricture, mass, raised nodule, ulceration, or a barely noticeable mucosal irregularity, such as a depression. EAC has been found in biopsy samples taken from Barrett's esophageal regions that appear flat under endoscopy. On occasion, smaller tumors are found that might respond to endoscopic treatment. Initial EAC treatment strategies depend on a number of variables, such as the stage and grade of the tumor, its location, the patient's age and comorbid conditions, as well as institutional therapeutic expertise [47]. It is critical to accurately identify patients who might qualify for curative endoscopic or surgical therapy for EAC, because systemic therapy is frequently ineffective in treating the condition. Patients with advanced disease often receive multimodal therapies, though its benefits have not yet been fully understood [2]. The standard of care for high-risk groups is endoscopic surveillance with biopsy evaluation, but before undergoing any of these procedures, it is important to take into account the patient's overall health and the risk of aspiration pneumonia, esophageal perforation, bleeding, or the development of tracheoesophageal fistulas [48].

Esophagectomy: while esophagectomy is a less common surgical option for treating superficial neoplasia, it is still a viable option in some circumstances. For instance, endoscopic therapy can still result in poor functional outcomes in patients with poor esophageal transit brought on by stricturing and aperistalsis. Esophagectomy can treat both the neoplasia and the compromised esophageal function in these cases. Esophagectomy for high-grade dysplasia or T1a cancer is associated with less than 3% mortality in tertiary care facilities [49]. But in more than 30% of esophagectomy patients, morbidity—most often in the form of pulmonary and wound infection—as well as anastamostic leaks do occur [50]. The standard course of treatment for patients with advanced but treatable esophageal cancers is surgery and chemo radiation, either in a neo-adjuvant or adjuvant setting [51]. In the US and the UK, esophagectomy is performed on more than 5000 patients annually, with

neoadjuvant therapy being used in 85% of cases [52]. The majority do experience complications, operative mortality is still quite high, and quality of life may be seriously compromised [53]. Despite the fact that the absolute survival benefit of neoadjuvant therapy ranges from 7% to 13% at 2 years [54], 50%–60% of tumors are resistant [55]. Neoadjuvant, adjuvant, and definitive chemo– and/or radiotherapy also carry risks.

Chemotherapy: it is used to treat EAC in a variety of situations. Neoadjuvant or perioperative chemotherapy is used for patients with operable disease to increase overall survival. The first study to show that chemotherapy in the form of cisplatin and 5-fluorouracil (5-FU) before esophagectomy increased 5-year overall survival from 17.1% to 23.0% was the Medical Research Council (MRC) OEO2 trial. Both esophageal squamous cancer and adenocarcinoma saw a survival benefit [48]. Chemotherapy is also used to enhance quality of life and extend survival in patients with metastatic, incurable disease.

Radiotherapy: Only more radiosensitive squamous cell cancers can be definitively treated for esophageal tumors with chemo-radiotherapy alone. However, it may be an option for EAC patients who are not candidates for surgical treatment or who choose not to receive it. Chemo-radiation has been used as a neoadjuvant treatment for esophageal cancer, and the CROSS trial has shown that it is superior to surgery alone in treating the condition [48]. However, squamous cell carcinoma accounted for the majority of these results, and adenocarcinomas were only marginally significant.

Targeted therapy: it is a type of cancer treatment in which drugs or other substances are used to identify and destroy specific cancer cells. Targeted therapies are less likely to harm normal cells than chemotherapy or radiation therapy. A type of targeted therapy known as monoclonal antibody therapy is used to treat esophageal cancer. As a cancer treatment, these antibodies can bind to a specific target on cancer cells or other cells, which may aid in preventing the growth of cancer cells. Proto-oncogene 5 encodes the human epidermal growth factor receptor (HER 2). This receptor is a member of the epidermal growth factor receptor family, and its phosphorylation causes cell division, proliferation, differentiation, and apoptosis. Drugs that target tumor cells that express the HER 2 protein have been shown to improve survival in breast cancer patients. An international phase 3 randomized clinical trial using trastuzumab, a monoclonal anti-HER 2 antibody directed against the HER 2 protein, was found to prolong survival in stomach and gastroesophageal junction adenocarcinomas that expressed HER2 [56]. It could be used to prevent the growth factor protein HER2 from

sending growth signals to esophageal cancer cells. However, because of the heterogeneity of the somatic alterations, a personalized approach appears to be required. New agents are being tested, including lapatinib, a dual epidermal growth factor receptor and HER2 tyrosine kinase inhibitor, and pertuzumab, another anti-HER2 antibody that has been shown to improve response rates in other cancers (e.g., HER2-expressing breast cancer) [48]. Tumors can only grow by recruiting a blood supply and angiogenesis; thus, molecular target could be also the tumor vasculature, as it is thought to have greater genomic stability and lead to a more predictable response. Ramucirumab, a monoclonal antibody against the vascular endothelial growth factor receptor (VEGFR) 2, was shown to improve overall survival in patients with gastric and GOJ adenocarcinomas when used alone or in combination with paclitaxel [48]. Preliminary research by our team suggested a link between *TP53* mutation status, recurrence, and survival of patients who underwent primary surgery (data not shown). We investigated a small number of EAC cases, which yielded promising results but left us underpowered in terms of the number of cases required to detect a significant association. Given that neoadjuvant cisplatin/fluorouracil chemotherapy requires a wild-type protein to be effective, *TP53* mutations are associated with poor response [57]. In contrast, pharmacological reactivation of mutant p53 using small molecules that restore its wild-type activity has emerged as a promising method for improving cancer therapy [58].

Classifications

One essential component of cancer diagnosis, treatment, and prognosis is an accurate classification. Assuming that cancers from the same site of origin shared similar pathogenic processes and therapeutic outcomes, tumor classification in the past relied on anatomical location and histologic features.

The Lauren classification

The Lauren classification is a widely used histopathological classification system that was initially created for gastric adenocarcinomas, and whose prognostic value has also been expanded to EACs to stratify patients (Figure 5):

- Intestinal type, which forms glandular structures resembling those of an adenocarcinoma of the large intestine and is typically well to moderately differentiated;
- Diffuse type, which has signet ring cells in varying proportions and is made up of poorly cohesive tumor cells with little to no gland formation;
- Mixed type carcinomas display characteristics of both diffuse and intestinal type carcinomas.

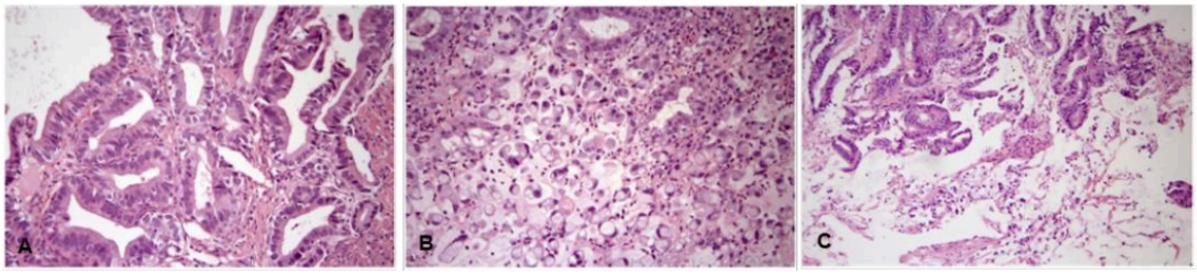

Figure 5: The three different subtypes of EAC according to the Lauren classification. Intestinal type, Diffuse type and Mixed type. *(From van der Kaaij et al., 2017)*

The Siewert classification

Based on the relationship between the location of the gastro-esophageal junction (EGJ) and the tumor's epicenter, Siewert and colleagues developed a classification system to divide gastro-esophageal junction (EGJ) adenocarcinomas into three types:

- Type I tumors, also known as distal esophageal tumors, have an epicenter that is 1 to 5 cm above the esophago-gastric junction and a bulk that is more than two thirds above the EGJ;
- Type II tumors (or true cardia carcinomas): the tumor epicenter develops between 1 and 2 cm above the EGJ;
- The epicenter of a type III tumor, also known as subcardial gastric carcinoma, is 2–5 cm away from the GEJ and infiltrates the EG junction and distal esophagus from below.

Due to the fact that these three types of tumors exhibit various lymphatic dissemination patterns, the Siewert classification is frequently used for preoperative assessment of the tumor location in order to plan the best surgical approach [59]. This classification method is still debatable because it ignores the molecular profiles and various biological behaviors that suggest that EAC may be consistently heterogeneous [5].

The EACSGE classification

The anatomo-pathologists in our research group recently created a novel histological classification based on the morphologic characteristics of esophageal/esophagogastric junction adenocarcinomas. Based on the growth pattern and cytostructural traits, seven morphologic subtypes with varying degrees of aggression were identified (Figure 6):

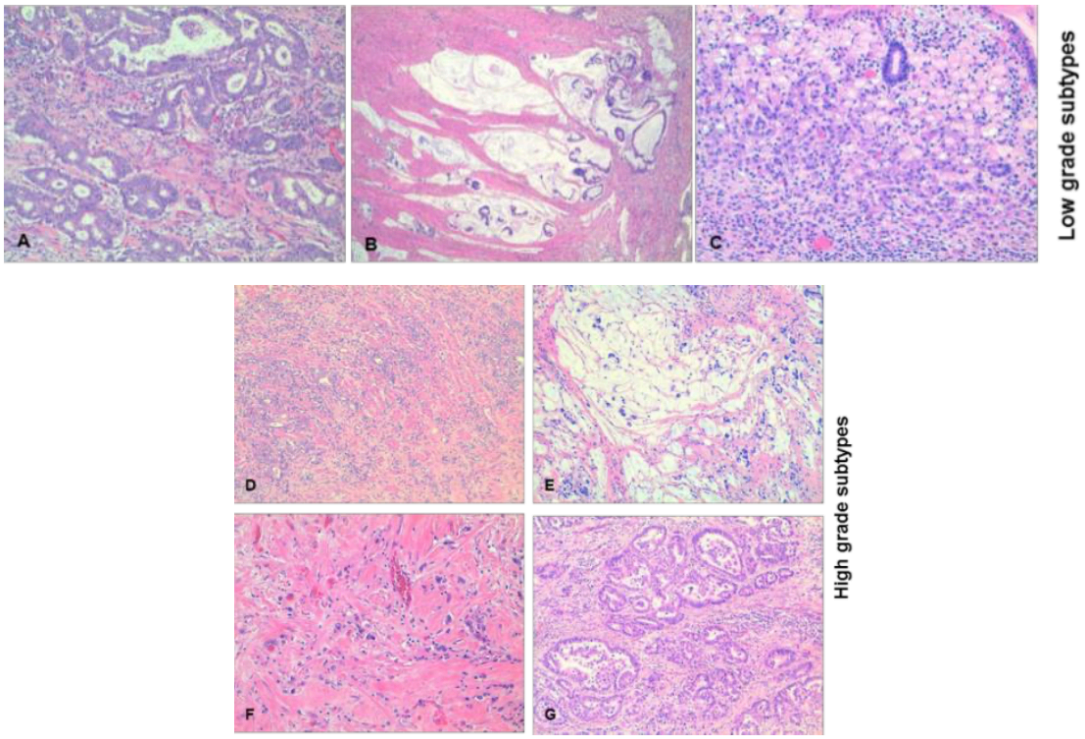

Figure 6: The EACSGE histologic classification. Haematoxylin eosin stain of EAC histotypes assigned according to the EACSGE classification. A. Glandular well differentiated; B. Mucinous well differentiated; C. Diffuse desmoplastic; D. Glandular poorly differentiated; E. Mucinous poorly differentiated; F. Diffuse anaplastic; G. Mixed. *(From Fiocca et al. 2020)*

- The term "glandular well differentiated" (GL-WD) refers to a tumor that retains its glandular structure throughout and exhibits little or no intercellular cohesion loss;
- Poorly Differentiated (GL-PD) Glandular Tumors: Intercellular cohesion is preserved but more than 10% of the glandular structure is lost;
- Mucinous Well Differentiated (M-WD): the tumor has at least 50% mucinous content, and its growth pattern is exclusively expanding;
- Mucinous Poorly Differentiated (M-PD) tumors have an infiltrative growth pattern and may exhibit signet ring characteristics. They are distinguished by the presence of weakly cohesive tumor cells floating in extracellular mucin lakes;

- Diffuse Desmoplastic (DD): Signet ring cells are typically restricted to the most superficial part of the tumor; poorly-cohesive cells infiltrate the wall and produce marked fibroblast-rich desmoplasia,
- Poorly cohesive cells with an infiltrative growth pattern and frequent angio-invasion are referred to as diffuse anaplastic (DA) and lack signet ring features;
- Mixed (Mix): an amalgamation of glandular and cellularly incoherent elements.

The Low Grade Carcinoma group, which includes the GL-WD, M-WD, and DD subtypes, and the High Grade Carcinoma group, which includes the GL-PD, M-PD, DA, and Mix subtypes, can be distinguished based on survival curves. Particularly when combined with stage, this classification has shown to have a statistically significant prognostic impact. Indeed, depending on the histologic subtype, the stage plus histotype combination has a high discriminating power for cancer-specific survival, ranging from 86.9% to 0% at 5 years [60].

Genomic signature of EAC: *TP53* gene

Overall, EAC patients have a poor prognosis; even after ostensibly curative treatment, 5-year survival is only 35%–45% [61], [62]. This demonstrates the gaps in our biological knowledge and the urgent need for biomarkers that can predict prognosis, recurrence, and sensitivity to therapy, ultimately allowing for more individualised care.

A high mutation frequency is a defining characteristic of EAC which exhibits various signatures through large-scale sequencing studies, including enrichment for the BRCA signature, frequent homologous recombination pathway defects, a dominant T>G mutation pattern linked to a high mutational load and neoantigen burden, and a C>A/T mutation pattern with evidence of ageing imprints [10].

Genome instability is thought to occur early in the development of EAC tumors [63]. Other genes, besides *TP53*, are altered in numerous EAC tumor samples, but less frequently. Therefore, classifying EAC patients into distinct mutational groups would enable targeted therapy by identifying the major mutational profile of these patients. By enabling customized preoperative care, markers that indicate the respond to chemotherapy would significantly increase treatment effectiveness. Protein expression with or without sequence changes has

been the focus of the majority of clinical experience with esophageal biomarkers to date; although these markers are used to choose patients for early phase trials, the only tumor marker currently used regularly is the presence of ERBB2/HER2 [64] However, the potential significance of somatic DNA sequence markers has been brought to light by the quick development of high-throughput next-generation sequencing (NGS). These could serve as standalone markers, be used to explore or improve on current expression markers, or be brand-new therapeutic targets [8], [65] The importance of germline variants in modulating cancer and treatment outcome has also been highlighted by developments in custom and genome-wide single nucleotide polymorphism (SNP) arrays [66]. According to some studies, p53 is crucial to know the patient's respond to various chemotherapeutic regimens. Drug resistance has been attributed to defective p53, allowing prediction of the response [67]. DNA damage is caused by chemotherapy drugs like cisplatin and fluorouracil which is the most potent inducer of p53 gene activation provoking the apoptotic cascade's genes activation, leading to a programmed cell death. However, this pathway is frequently obstructed because *TP53* is the most frequently mutated gene linked to cancer [68].

New potential marker in EAC: *HNF1alpha* gene

Initially identified as liver-enriched transcription factors that could have multiple functions in the transcription of genes specific to the liver, hepatocyte nuclear factors (HNFs) were discovered. Nevertheless, it became clear over time that HNFs are not just found in the liver. Since then, it has been discovered in the keratinocytes and melanocytes of human skin, as well as the pancreas, kidneys, intestine, spleen, and thymus [69].

The 12q24.2-located hepatocyte nuclear factor 1 homeobox A gene, which has 9 exons, encodes for transcription factor HNF1alpha, a member of the HNF1 homeobox family. There are three isoforms of HNF1alpha: A (encoded by exons 1–10), B (exons 1–7), and C. (exons 1–6). [70], [71].

As showed in figure 7, HNF1alpha is structurally composed of 631 amino acids and has three functional domains: an N-terminal dimerization domain (between residues 1 and 32), and a bipartite DNA-binding motif with an unusual POU-homeodomain (between residues 98 and 280) and a C-terminal transactivation domain (between residues 281 and 631) [69]–[71]. The

POU homeodomain (POUH) and POU-specific (POUS) components constitute the DBD, which is known to bind to the palindromic consensus sequence GTTAATNATTANC.

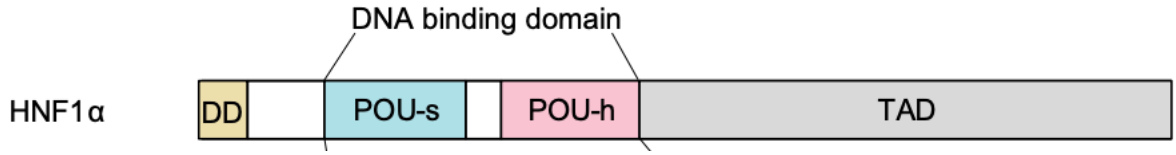

Figure 7: A schematic diagram of HNF1a. The N-terminus consists of the DD. The DBD of the family is made up of a POU-s and a POU-h. The C-terminus contains the TAD which is less conserved between the two members of the HNF1 family. *(From Lau et al. 2017)*

HNF1alpha expression and function

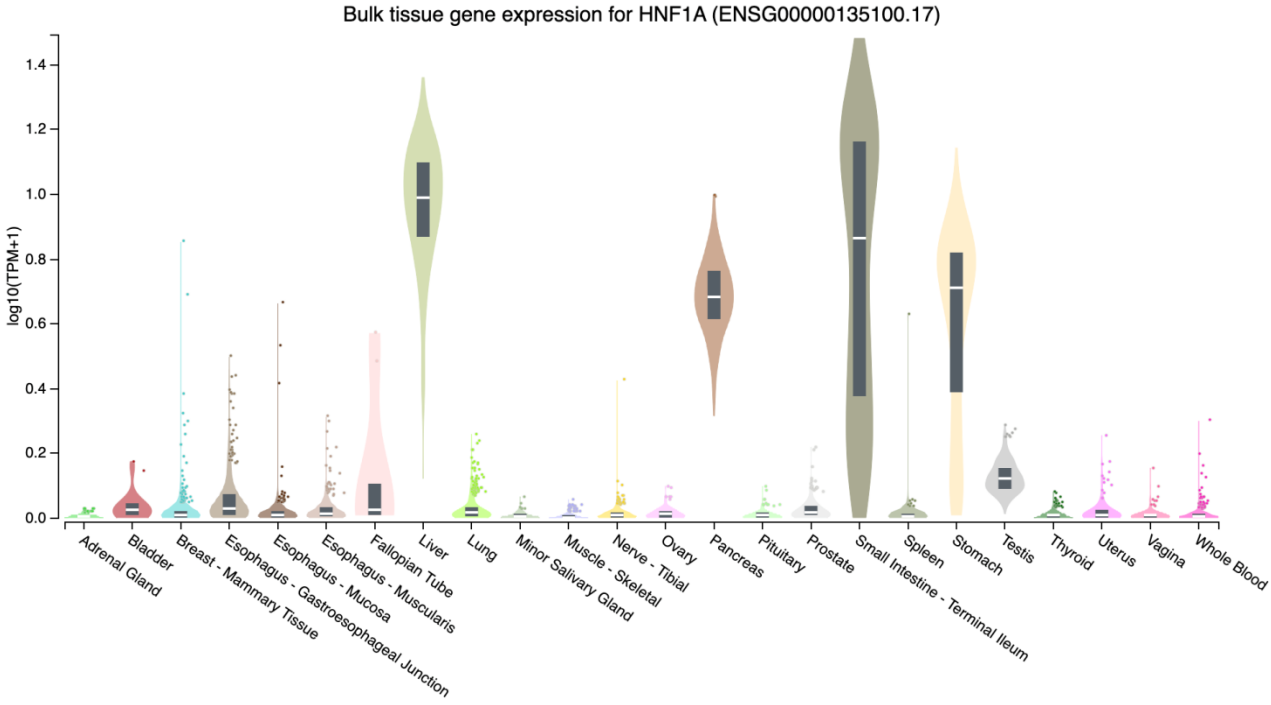

Figure 8: Tissue gene expression for HNF1alpha via https://gtexportal.org/home/gene/HNF1A

Through transcription, HNF-1 carries out a number of significant processes primarily connected to cellular homeostasis and metabolism in crucial organs. Cell lineage differentiation, lipid metabolism, glucose metabolism, angiotensin-converting enzyme 2 (ACE2), pancreatic development, β-cell growth, proteins involved in type II diabetes, bile acid transporters in the kidneys, and drug metabolism have all been reported to be affected so far. [69]. Additionally, HNF1alpha plays a significant role in the transcriptional networks that control the growth and differentiation of the embryonic pancreas as well as the maintenance of adult islet cell growth and function [71]. Human-specific long non-coding RNA (LINKA)

is decreased when HNF1alpha is lost in beta cells derived from human embryonic stem (ES) cells, which suggests that HNF1alpha is involved in mitochondrial function [70] [72].

Aspirin and resveratrol have been identified as potential exogenous ligands in silico analysis, whereas the endogenous ligands of HNF1alpha are unknown [70]. Specifically, the liver, gut, pancreas, and kidneys express HNF1alpha. It plays a variety of roles in human cells, and because it is tissue-specific, it performs various tasks in organs. It functions as a tumor suppressor, aids in protein synthesis, and regulates lipid metabolism in the liver (Figure 9).

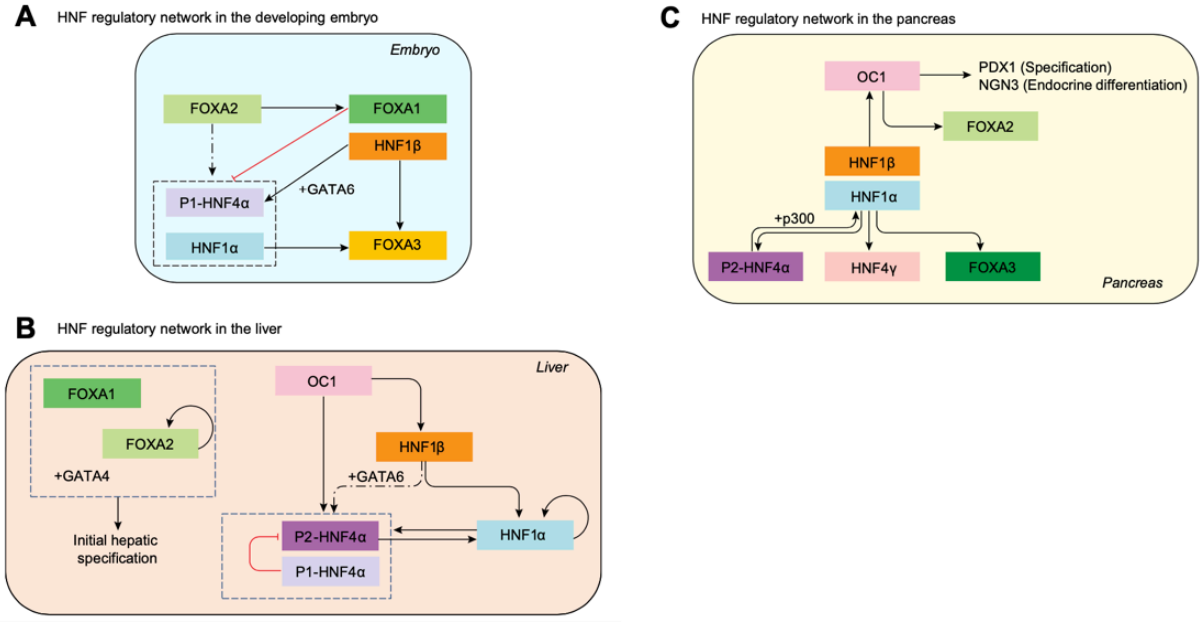

Figure 9: Schematic outlining key HNF1 alpha cross-regulatory networks. (A) HNF4a and HNF1a, both driven by P1, have their gene expression negatively regulated by FOXA1. positively regulate FOXA3. HNF1b and GATA6 work in concert to tightly control the expression of P1-driven HNF4a. (B) The liver's HNF regulatory network. The initial specification of liver progenitors involves FOXA1, FOXA2, and GATA4. Further controlling its own expression, FOXA2. (C) HNF1a is also involved in regulating the expression of HNF4a, HNF4c and FOXA3 transcripts in islets. *(From Lau et al. 2017)*

Indeed, homozygous HNF1alpha-deficient mice showed growth retardation and hepatomegaly [70], indicating that lipid metabolism plays a crucial role in liver function. Along with altered gene expression related to the synthesis and uptake of bile acids and de novo biosynthesis of cholesterol, *HNF1alpha*-null mice also had hyperbileacidemia and hypercholesterolemia [70]. A remarkably large number of genes involved in the glycolytic pathway, the tricarboxylic acid (TCA) cycle, and mitochondrial oxidative phosphorylation showed decreased expression levels in *HNF1alpha-/-* islets in contrast to *HNF1alpha*-deficient liver, which displayed increased expression levels of genes regulating glycolysis and gluconeogenesis. [71].

While *HFN1alpha* expression was weak in duct cells, it was found in the majority of pancreatic epithelial cells, hormone-positive cells, and amylase-positive cells [73]. In mouse islets, HNF1alpha is necessary for the upkeep of histone acetylation in the promoter regions of its target genes, including *GLUT2* [70]. *SGLT1* expression in mouse alpha cells was directly regulated by HNF1alpha, which was involved in glucagon secretion during hypoglycemia [74]. Hypoglycemia and impaired insulin secretion in *HNF1alpha*-null mice suggested that HNF1alpha was involved in the secretion of insulin by mouse beta cells [75]. Heterozygous mice lacking HNF1alpha, however, have normal blood sugar levels [76]. Double knock-down of the *HNF1alpha* gene in mice causes multiple symptoms such as hepatomegaly, phenylketonuria, Fanconi syndrome, and noninsulin-dependent diabetes mellitus [77]. In summary, HNF1alpha is involved in multiple metabolic pathways which play an important role in maintaining normal metabolism of the body. However, its regulation mechanism is still unclear (Figure 9).

MODY3 (Maturity-Onset Diabetes of the Young Type 3)

MODY is a distinguished autosomal dominant form of diabetes with onset before the age of 25, and impaired insulin secretion due by mutations in transcription factors involved in beta cell differentiation and function [70], [71]. To date, 14 MODY subtypes have been reported, including MODY1 (HNF4A), MODY2 (GK), MODY3 (HNF1alpha), MODY4 (PDX1), MODY5 (HNF1B), and MODY6 (NeuroD1). Among these, *HNF1alpha* gene mutations are the most common cause of MODY [70].

P291fsinsC, the most prevalent HNF1alpha mutation in MODY3, negatively affects wild-type HNF1alpha by removing the majority of the transactivation domain [70]. *Hnf1*-null (-/-) mice and transgenic mice displaying a naturally occurring human dominant-negative P291fsinsC *HNF1alpha* gene variant in pancreatic β-cells showed an increase in the risk of diabetes at a young age, with impaired insulin secretion and a decrease in β-cell number [74]. According to these findings, HNF1alpha is necessary for healthy insulin secretion and β-cell maintenance. The amino-terminal dimerization and DNA-binding domains are frequently affected by missense mutations, while the transactivation domain is frequently affected by deletion mutations, potentially resulting in clinical heterogeneity in MODY3 patients [70]. With the exception of one variant from the Bergen dataset (p.Arg131Gln, 50%) and five from the Oxford dataset (p.Asn62Ser, c.340C>T [p.Arg114Cys], c.467C>T [p.Thr156Met], c.481G>A

[p.Ala161Thr], p.Ser535Arg *50%*), the subsets of variants investigated by EMSA demonstrated overall normal DNA binding ability [78]. As seen in HNF1alpha-deficient models, *HNF1alpha* mutations (MODY3) reduce insulin secretion by altering glucose metabolism in beta cells [71]. This is linked to the downregulation of specific glucose metabolism genes such as glucose transporter 2 (GLUT2) and glucose uptake [70]. Furthermore, the most common HNF1alpha mutation in MODY3 (P291fsinC) decreases mitochondrial ATP production in mouse beta cells, resulting in ATP production and subsequent insulin secretion [70].

Researchers discovered deeply reduced expression in HNF1alpha-/- islets in over 20 genes associated to glycolysis, oxidative phosphorylation, and the source of amino acids for the TCA cycle [74], [79]. Malic enzyme 3 (Me3) and fumarate hydratase (Fh1), two essential TCA cycle enzymes, are likely to be downregulated, which may contribute to the defective mitochondrial metabolism [80].

HNF1alpha gene in cancer

There have been reports of *HNF1alpha* mutations in 35–40% of patients with hepatocellular adenoma (HCA). In contrast to MODY3, bi-allelic inactivation of *HNF1alpha* has been found in tumor tissue. This is frequently caused by two inactivating somatic mutations, though on rare occasions one inactivating germline mutation may also be present along with a second inactivating mutation [81]. These findings imply that *HNF1alpha* might function in the liver as a tumor suppressor gene [77][78]. Increased tissue glucose uptake, which can worsen the carcinoma phenotype, is also connected to *HNF1alpha* mutations. The potential mechanism of HNF1alpha-inactivated HCAs (H-HCAs) was clarified by Ozaki et al., who discovered increased glucose uptake largely as a result of *GLUT2* and *HK4* increased expression and *G6PT1* inactivation [84]. HNF1alpha has established a solid reputation as a promising drug target for HCC, in addition to its regulatory function in hepatic lipid and glucose metabolism. Additionally, data from genome-wide association studies (GWAS) have connected HNF1alpha to a higher risk of pancreatic cancer [85]. Multiple hotspot mutations in *HNF1alpha* have been discovered in liver cancer through high-throughput analysis of cancer cell genomes. These findings also highlight HNF1alpha as a crucial therapeutic target for the approach of personalized medicine (Figure 10) [72].

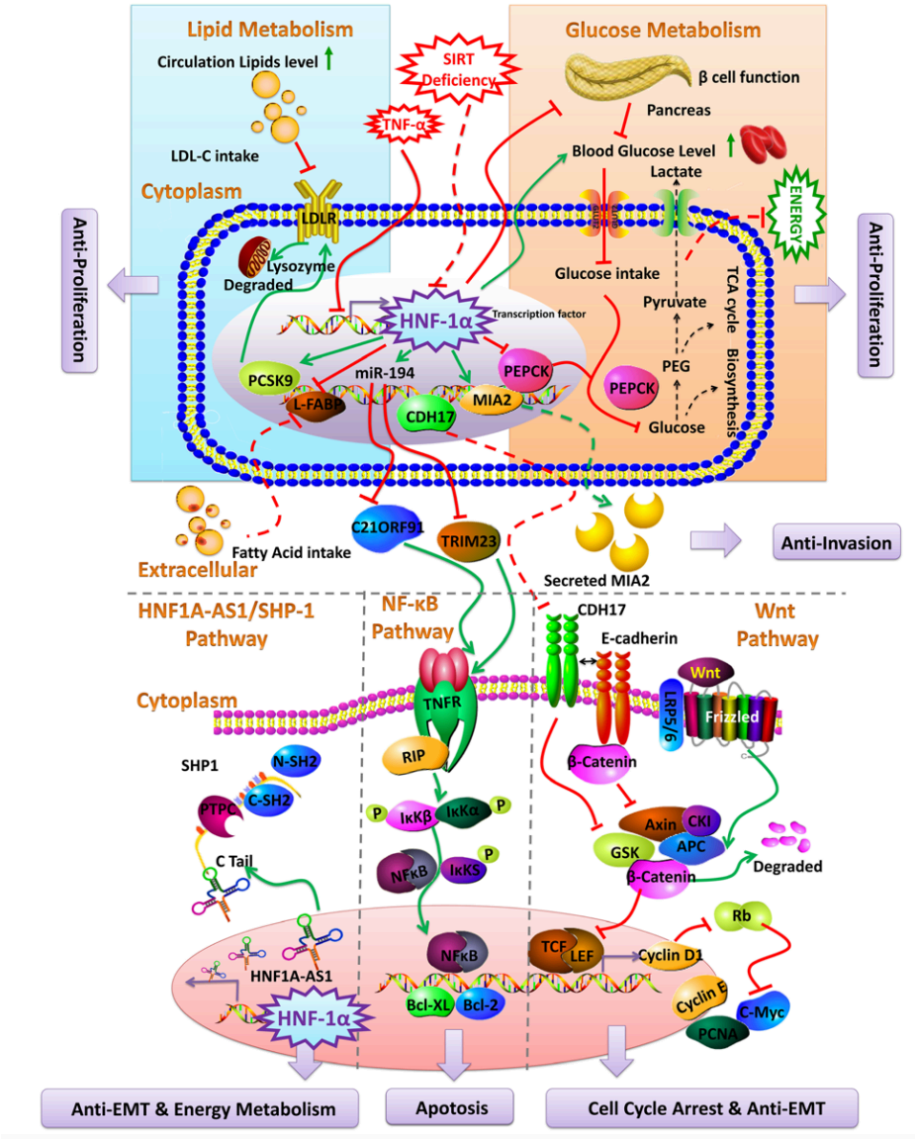

Figure 10: Schematic outline of the reported metabolic background of HNF-1α regulatory mechanism networks in various types of liver malignancies. *(From Wang et al. 2019)*

The overexpression of several genes encoding growth factor receptors, parts of the translational machinery, cell cycle, and angiogenesis regulators was upregulated by siRNA-mediated *HNF1alpha* silencing in hepatocellular carcinoma cells [83]. These results suggest that HNF1A may influence the development of cancer by controlling immune function, inflammatory response, protein folding, and cell growth and differentiation. Additionally, marked steatosis with aberrant mTOR pathway activation characterized *HNF1alpha*-mutated hepatocellular adenomas (H-HCAs). These tumors also showed an increase in the protein and mRNA levels of the protein translation enzymes eIF-4G3 and eEF1A2. Moreover, cyclin D1 and eIF-4G3 were found to be strongly correlated with the expression of HNF1alpha at the protein level [83] in the same study. Hepatic steatosis brought on by increased fatty acid

synthesis and decreased expression of liver fatty acid-binding protein is a well-known marker associated to the mutations of *HNF1A* in HCA (LFABP). Dysregulated gluconeogenesis, glycolysis, and lipogenesis are the metabolic effects of biallelic *HNF1alpha* mutations [86]. Increased ErbB2 receptor tyrosine kinase activity leads to neoplastic consequences by activating the mTOR signaling pathway, which has pro-proliferative and anti-apoptotic effects [87], [88]. The absence of β-catenin activation, *CTNNB1* (Catenin Beta-1) mutations, and impaired HNF1A signaling are the hallmarks of HCAs [89]. Hechtman et al. [90] identified two mutations in HCC: HNF1alpha p.E32X and p.L214Q. The HNF1alpha p.Q511L somatic mutation was discovered in HCC by Ding et al. [86] and was characterized by decreased transactivation activity and compromised nuclear localization of HNF1alpha. The hepatocellular carcinoma epithelial phenotype is compromised by the silencing of HNF1alpha by siRNA, as evidenced by the decreased expression of epithelial markers like E-cadherin and the increased expression of mesenchymal markers like vimentin and transcription factors (TFs) involved in EMT like Snail1 and Snail2 [72], [91].

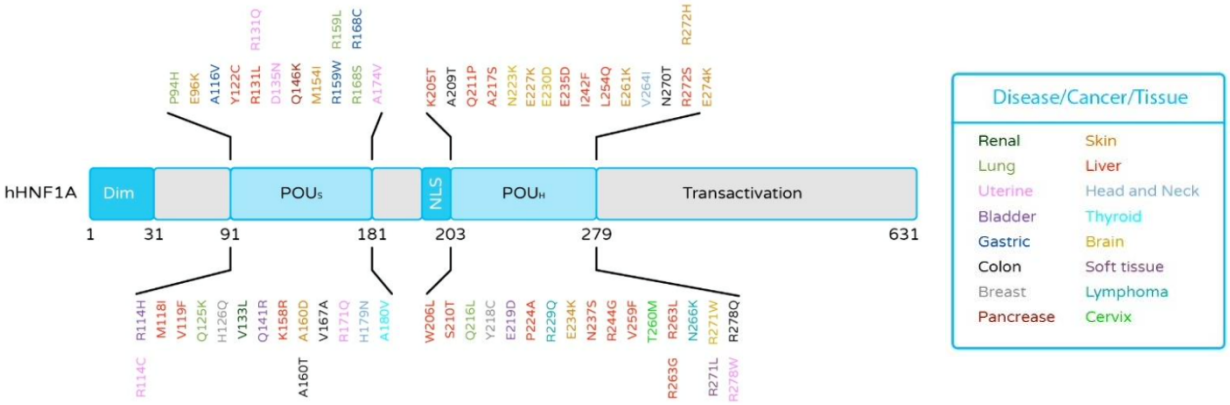

Figure 11: HNF1alpha mutations are found in the DNA-binding domain (DBD) in several cancers identified by the International Cancer Genome Consortium (ICGC). The amino acid positions of the identified mutations of HNF1alpha are shown, and the color coding indicates the type of cancer tissue in which the mutations were reported. *(From Teeli et al. 2021)*

According to a recent study, pancreatic cancer stem cells (PCSCs) have high levels of HNF1alpha expression, which raises the possibility that HFN1A functions as a key regulator of PCSC function [92]. In that study, HNF1alpha knockdown inhibited tumor growth and induced apoptosis in a manner that was accompanied by a decrease in stem cell markers in a number of PDAC cell lines. On the other hand, HNF1alpha overexpression accelerated the rise of stem cell markers and promoted tumor growth in PDAC cell lines. The rate of pancreatic cancer cell proliferation was also increased by silencing HNF1alpha expression

[82]. In fact, Patitucci et al. demonstrated that AKT2 phosphorylated and inhibited HNF1alpha, with the suppression of hepatic PPAR expression and consequently encouraged tumorigenesis [93]. It was confirmed once more that there is a connection between HNF1alpha inactivation and various tumor-promoting and developmental mechanisms. In keeping with earlier findings, HNF1alpha inactivation demonstrated increased lipogenesis and induction of glycolysis in addition to the activation of the mTOR pathway [83]. These findings suggest that HNF1alpha activation in pancreatic cancer promotes tumor growth, despite evidence that the protein also inhibits tumor growth in this disease [94], [95].

According to a different study, HNF1alpha inhibition in liver cancer cell lines resulted in the loss of cell-cell contacts and the formation of migration structures with the upregulation of TGFB1, SNAIL, and SLUG, indicating that EMT is prompted by the loss of HNF1alpha expression [96]. The activation of the Akt signalling that causes liver pathology significantly increases PPARG expression in human liver cancers. HNF1alpha is no longer functional in liver lesions, which causes PPARG expression and tumorigenesis [80].

HNF1A was found to play a tumor suppressor role in multiple cancer cell lines, but little is known about the extent to which its function varies in tissues, particularly the esophagus and its adenocarcinoma, and the underlying transcriptional mechanisms.

Aims of the study

A better definition of EAC mutational status and inter- and intra-tumor heterogeneity will improve the understanding of the molecular architecture of the different cell populations in the primary EAC tumors, i.e. the tumor clonality, and will allow to evaluate the predictive role of biomarkers.

- Therefore, I aimed to achieve molecular and transcriptional profile definition of a large collection of EAC cases by using next generation sequencing (NGS) of extracted DNA and RNA, to correlate the presence of specific variants and gene signatures with histological subtypes and clinical outcomes.
- I also wanted to perform *in vitro* analysis of the novel variants in *HNF1alpha* in gene-edited esophageal cells, to evaluate their contribution to cancer development and progression in term of cell proliferation, cellular metabolic functions, anchorage independent growth and invasion.

Materials and methods

Sample recruitment

The 164 DNA samples used for the analysis derived from EAC patients who underwent surgery at the following facilities: Istituto Europeo di Oncologia (IEO), Milano (14 cases); IRCCS Ospedale San Raffaele, Milano (127 cases); and Ospedale di Verona, Verona (23 cases). The presence of esophagogastric junction adenocarcinoma and the absence of neoadjuvant therapy (chemo-radiotherapy-naive EACs) served as the inclusion criteria. All surgical re-sections underwent formalin fixation and paraffin embedding (FFPE), gastrointestinal pathologists analyzed them, and they were all categorized in accordance with the EACSGE histological classification [60].

Custom EAC Panel: library preparation, hybridization and sequencing

Using the QIAMP DNA FFPE Tissue Kit (Cat. 56404; Qiagen Hilden, Germany), DNA was extracted from two 40-m thick, FFPE sections in accordance with the manufacturer's instructions. The Lotus DNA library prep kit (Cat. 10001074; Integrated DNA Technologies IDT Inc. Coralville, USA) was used to create dual-index paired-end libraries in accordance with the manufacturer's instructions for the enrichment of 26 oncology-related genes (reported in Table 1). An enzymatic preparation (where 300–350 bp DNA fragments were obtained and end-repair and dA-tailing were performed), the ligation of stubby adapters, and PCR amplification for 11 cycles with indexing primers comprised the protocol's three main steps (to incorporate sample-unique indexing sequences and P5 and P7 sequences to attach to stick to the flow-cell). Using the Qubit dsDNA BR Assay Kit, the single DNA libraries were quantified after being purified and run on a 3% agarose gel to confirm the proper size (Cat. Q33265; ThermoFisher Scientific Vilnus, Lituania). To perform hybridization and enrichment for particular gene regions, 500 ng of each library preparation was pooled in groups of 16 samples. In accordance with the protocol, this step was performed using xGen Lockdown probe pool and xGen hybridization capture of DNA libraries kit (IDT). Each pool of 16 samples underwent 16 hours at 65 °C of hybridization to the capture probes. Individually synthesised, 5′ biotinylated oligos known as xGen Lockdown Probes were put together in a custom panel of 28 genes for target capture. Genes selected for this study are listed in Figure 12. After removing the unbound products from the hybridised regions and capturing them with streptavidin magnetic beads, an 11-cycle post-capture PCR was carried out. The Qubit dsDNA HS Assay kit (Cat. No. Q33230; Thermo Fisher Scientific) and 2100 Bioanalyzer

High Sensitivity DNA (Agilent Technologies) were used to measure the quantity and size of the enriched library pools. On an Illumina NextSeq 500 platform (Illumina San Diego, USA), each pool was normalised to 1.3 pM before being sequenced at 150 bp paired ends. An in house-pipeline programme was used for data analysis [97]. The bioinformatic tool BWA-MEM was used for alignment of sequenced library (hg19 as reference human genome). For calling variants, we used GATK tool packs and an in-house tool called "Rabdomyzer" (not published) was used for the initial prioritization of variants based on the minor allele frequency values (MAF) and Variant Ontology Terms. Other criteria of prioritization were the CADD, PolyPhen-2 and SIFT scores for the different variants [97], [98].

Table 1:

GENE	REFSEQ NM	REFSEQ NP
TP53	NM_000546	NP_000537
ATM	NM_000051	NP_000042
PI3KA	NM_006218	NP_006209
CDKN2A	NM_000077	NP_000068
PTEN	NM_000314	NP_000305
MET	NM_000245	NP_000236
MSH6	NM_000179	NP_000170
IDH2	NM_001289910	NP_002159
APC	NM_000038	NP_000029
TSSC1	NM_003310	NP_003301
ERBB2	NM_004448	NP_004439
HNF1A	NM_000545	NP_000536
FLT3	NM_004119	NP_004110
STK11	NM_000455	NP_000446
SMAD4	NM_005359	NP_005350
ALK	NM_004304	NP_004295
CHEK2	NM_001005735	NP_001005735
KRAS	NM_004985	NP_004976
SMARCA4	NM_001128844	NP_001122316
CDK6	NM_001145306	NP_001138778
RET	NM_020630	NP_065681
MAP2K1	NM_002755	NP_002746
EGFR	NM_005228	NP_005219
CTNNB1	NM_001098209	NP_001091679
ARID2	NM_152641	NP_689854
SRC	NM_198291.3	NP_938033.1

Immunohistochemistry

Hematoxylin-Eosin (HE), TP53, and HNF1A antigen immunohistochemistry were carried out automatically with Benchmark XT® immunostainer (Ventana Medical Systems). Positive controls (such as an external positive control put on the slide) and negative controls were used to validate the immunohistochemical analysis (by omitting the primary antibody). Immunohistochemistry (IHC) was used to analyze surgical specimens embedded in paraffin to identify cases with predicted harmful variants in HNF1A. Two independent evaluations were performed for each IHC of TP53 and HNF1A. The results were scored blindly to the presence or absence of mutations. As controls, cases without gene variants were used.

RNA analysis

RNA was obtained out of the FFPE samples (5 for each EACGSE subgroup). The samples that had a good RNA Integrity Number (RIN) score and a DV200 > 40% were chosen for further analysis. Following the manufacturer's instructions, libraries were created starting from 100 ng of 27 RNA using the TruSight RNA Pan-Cancer Panel Kit (Illumina, San Diego, California, USA; 1385 cancer-associated genes). Paired-end RNA-sequencing (Reagent Kit v3 -150 cycles, MiSeq, Illumina) was carried out on 22 libraries that passed protocol quality checks, and the raw sequencing data were converted to FASTQ file format and analyzed using FusionCatcher (FC(1)), STAR-Fusion (SF), and two Basespace applications [RNA-Seq Alignment v.1.1.0 (RSA), and TopHat Alignment v.1.0.0 (THA); Illumina]. All the aligners used the reference "Homo sapiens UCSC hg19 (RefSeq and Gencode gene annotations)". We kept the fusions that were found using three or more tools, and we added new standards to determine whether to keep or refuse the presence of gene fusions found using two or one tool. Sanger sequencing was used to confirm the gene fusions as previously described [97].

Cell lines

HNF1alpha expression was measured in OE-19, OE-33 and FLO-1 cell lines. All cells were cultured at 37°C in a 5% CO_2 incubator. For functional studies, the OE-19 cell line (ECACC: 96071721) [99], [100] was used, which was derived from a primary gastric cardia/esophageal gastric junction adenocarcinoma in a 72-year-old male patient. At pathological stage III (UICC), the tumor displayed moderate differentiation [192], [193]. At 37°C in a 5% CO_2 atmosphere, OE-19 were cultured in Roswell Park Memorial Institute (RPMI)-1640 medium (EuroClone) supplemented with 10% fetal bovine serum, 100 U/ml penicillin and 100 g/ml streptomycin (supplements from SigmaAldrich, St. Louis, Missouri, USA).

Basal mRNA expression of HNF1alpha in cell lines

Following the manufacturer's instructions, total RNA was extracted from cultured cells using Trizol reagent (Life Technologies, Grand Island, NY). 1.0 µg of total RNA was used to create complementary DNA with the cDNA Synthesis Kit (Bio-Rad Laboratories, Hercules, CA). Using specific primers designed with the program Primer3, triplicate samples were run through quantitative RT-PCR (qRT-PCR). HNF1alpha F: 5′-ACTCCCATGAAGACGCAGAA-3′, HNF1alpha R: 5′-TTCTTGGTTGGTAGCTCATCAC-3′, human Actin-beta F: 5′-CCTGGCACCCAGCACAAT-3′, human Actin-beta R: 5′-GGGCCGGACTCGTCATACT-3′. The qRT-PCR was performed in triplicates using the SYBR Green kit (QIAGEN) in a StepOne Plus Real Time PCR system (Thermo Fisher). The qRT-PCR results were first normalized to the threshold cycle (Ct) of Actin-beta (act-B), referred to as ΔCt. Gene expression in the cell lines as compared to a commercial pool of normal esophagus RNAs from 5 different donors (BioChain, Newark, CA, USA) was expressed as a fold change using the 2-ΔΔCt method [101].

Sanger sequencing

Sanger sequencing was used to check the status of HNF1alpha in EAC cell lines. Following the manufacturer's instructions, PCR amplification was carried out using KAPA HiFi HotStart (Hoffman-La Roche) beginning with the extracted genomic DNA. The primers that were used are listed in Table 2. Following purification using 96-well multiscreen PCR (Millipore), PCR products were sequenced in the 2720 Thermal Cycler using the BigDye v1.1 kit from ThermoFisher Scientific (ThermoFisher Scientific) under the following conditions:

Hold	96°C	1’
35 cycles	96°C	10”
	60°C	4’

Purified sequencing reaction products were run on a 3730 DNA Analyzer using Montage SEQ 96 plates from Millipore (Thermo Fisher Scientific). Electropherograms were visualized with Sequencer 4.7 (Gene Codes Corporation, Ann Arbor, MI, USA) or Chromas 2.0, (Chromas, Technelysium, South Brisbane, Australia).

Table 2: Primers pairs used for HNF1alpha analysis

HNF1a-ex1F	CAGGCAAACGCAACCCAC
HNF1a-ex1R	GGGACTCAACTCAGAAGGGG
HNF1a-ex2F	CTTTCATGCACAGTCCCCAC
HNF1a-ex2R	TGTCTGTGTAATGGGGATGGT
HNF1a-ex3F	AATCAAGGGCAAGGTCAGGG
HNF1a-ex3R	CCAATATCAGGAGTTCTCGGC
HNF1a-ex4F	TCTCAGAACCCTCCCCTTCA
HNF1a-ex4R	GACAGTCCTCCCCAACCC
HNF1a-ex5F	GGAGTTTGAAGTGCTGAGGG
HNF1a-ex5R	TCCAGAATCTCCCTGCCAAG
HNF1a-ex6F	CCAACCTCATCTTTCCTTGGC
HNF1a-ex6R	ATGAATGAGTCCCAGTGGCT
HNF1a-ex7F	AGGGGTGGGATATAACTGGG
HNF1a-ex7R	TGACAGCCAACCTCTATCATCA
HNF1a-ex8/9F	GATCTCCAACTGCTGCCCA
HNF1a-ex8/9R	GTGACGGACAGCAACAGAAG
HNF1a-ex9F	GGCCCAGTACACCCACAC
HNF1a-ex9R	GGGCAGGGACAGTAAGGG
HNF1a-ex10F	CTAGGGACAGGCAGGTGG
HNF1a-ex10R	CTGCTGCCCTCATCACCC

Mitochondria network staining and count the amount of mitochondria

OE-19 e FLO-1 cell lines were plated at a density of 5×10^5 cells/ well. When the cells reached the desired confluency, the media was removed and a prewarmed (37°C) staining solution containing 200 nM of MitoTracker Green FM Thermo Fisher) was add in each dish. The cells were incubated for 30 minutes and a wash was performed with fresh media. The pictures were taken with fluorescence microscopy using the Leica SP8 microscope.

A real-time qRT-PCR was performed in OE-19 and FLO-1 cell lines to evaluate the amount of mitochondria using primers for genomic DNA (gDNA) and for mitochondria DNA (mtDNA): B2M F: 5′-CCACCCACCTCAGATAGAA-3′; B2M R: 5′-TGTGAGCCAGGATGTAGGA-3′; MTND1 F: 5′-CCACCTCTAGCCTAGCCGTTTA-3′; MTND1 R: 5′-GGGTCATGATGGCAGGAGTAAT-3′; MTND2 F: 5′-CCCATACCCGAAATGTTGG-3’; MTND2 R: 5′-CTCAAATTCTGCCGGGGCTTCT-3′. We followed the protocol of RNA extraction and qRT-PCR as described previously.

siRNA blocking

Small interfering RNA (siRNA) transfections were performed using TransIT®-LT1 Transfection Reagent according to the manufacturer's protocol (Mirus Bio LLC). Three different siRNA targeting HNF1ALPHA gene (NM_000545) were tested. The sequences of the siRNAs (pre-designed siRNAs, Origene) are as follows:

- SR321977A 5'-rCrCrUrUrCrUrUrGrGrUrUrGrGrUrArGrCrUrCrArUrCrArCrCrUrG-3' (siRNA A),
- SR321977B 5'-rGrUrUrCrCrArArGrUrArArGrArArGrArCrUrGrUrArUrCrCrCrArC-3' (siRNA B),
- SR321977C 5'-rUrCrArGrUrUrUrArGrArArArCrCrArUrGrGrCrUrCrGrGrCrUrGrC-3' (siRNA C).

A negative control siRNA or transfection reagent only was used in mock transfections. OE-19 cells were transfected and after 48 hours the transfection was performed again. After 96 hours of transfection, RNA and proteins were collected and SeaHorse analysis was performed (see above).

Quantitative reverse transcriptase real time PCR (qRT-PCR).

Total RNA was extracted from OE-19 cell lines using the RNeasy Plus Mini Kit (Invitrogen) and RNA concentration and quality were verified using a NanoDrop 2000 spectrophotometer (ThermoFisher Scientific). cDNA was prepared using the Maxima First Strand cDNA synthesis Kit for RT-qPCR with DNase I (Thermo Fisher). Human specific primers for *HNF1alpha, Actin-beta, Ki67, GLUT-1* were used. (primers for HNF1alpha and actin-beta see above). KI67 F: 5′-TCCTTTGGTGGGCACCTAAGACCTG-3′; KI67 R: 5′-TGATGGTTGAGGTCGTTCCTTGATG-3′; GLUT-1 F: 5-′CAGCTGTCGGGTATCAATGC-3′; GLUT-1 R: 5′-AACAACATCTCGCTCGACCT-3′. The data from qRT- PCR was analyzed using comparative Ct method as described earlier.

Western blot analysis

Mammalian protein extraction reagent (M-PER) was used to extract proteins from cultured cells (Invitrogen). The BCA method was used to quantify the extracted proteins at 490 nm. Proteins were resolved using Stain Free SDS-PAGE and then transferred onto nitrocelluse membrane with the Midi transfer Pack (Biorad). The membranes were blocked with 5% BSA

(Sigma-Aldrich Corporation), for 45 min and then ere incubated 16 hours at 4°C with primary antibodies (1:500 for HNF1alpha SantaCruz Technologies, 1:1000 for Akt-PAkt-mTOR-PmTOR Cell-signaling; a total protein was used as control). The membranes were washed 3 times with TBS-T, followed by a 1 hour incubation with the respective secondary horseradish peroxide-coupled antibodies (1:1000 α-mouse, 1:1000 α-rabbit, Sigma-Aldrich). The expression levels of proteins from various treated groups were measured using enhanced chemiluminescence.

Extracellular flux analysis (Seahorse method)

One million of OE-19 cell lines were transfected for 72 hours with siRNAs against HNF1alpha (see before). After that period, OE-19 cells were seeded at a density of $3x10^4$ cells/well into an XF96-well plate in RPMI containing 25 mM glucose. After 24 hours, the cells were grown for 1 hour in an incubator CO_2-free and then the plate was transferred into the Seahorse machine, and after the completion of calibration, the program was started. After four measurement cycles of basal cellular respiration, cells were stimulated with serial injections of olygomycin (2 mg/mL, 3 cycles) followed by Carbonyl cyanide-4-(trifluoromethoxy) phenylhydrazone FCCP (0.3 μM, 3 cycles), and additional FCCP (0.2 μM, 3 cycles), and a mixture of rotenone/antimycin A (R/A; 1/2 μM, 2 cycles). Oxygen consumption rates (OCR) and extracellular acidifications rates (ECAR) were measured using a XF96 Extracellular Flux Analyzer (Agilent, Santa Clara, CA, USA). For normalization, the DNA content of the cells was measured with DAPI staining. The individual bioenergetics parameters of OXPHOS were calculated as previously described [102]. We performed also experiments with FLO-1 cell lines without HNF1alpha silencing, to better understand the differences between the two cell lines.

Statistical analysis

Data were analyzed using SPSS (version 15.0; SPSS Inc., Chicago, IL, USA) or Prism (Graph Pad Software Ins., California, USA). Differences in frequency data were analyzed using Chi-square ($\chi 2$) or Fisher's tests as appropriate. Mann-Whitney test was used to analyze continuous variables. P-values <0.05 were considered significant.

Results

Genetic changes discovered in EAC samples

A high-throughput sequencing was performed in 164 EAC samples with a custom panel of 26 cancer-related genes that were selected because of previous mutation screening data in a small cohort of EAC cases [97]. We considered variants of good quality in vcf file (LOF: nonsense and splice variants, missense) and selected the rare variants with parameters like MAF <0.005 (0.5%), CADD>15. A total of 337 variants were identified across the whole cohort (Figure 12). The most frequent variations (82.21%) were point mutations, followed by insertions and deletions (17.78%).

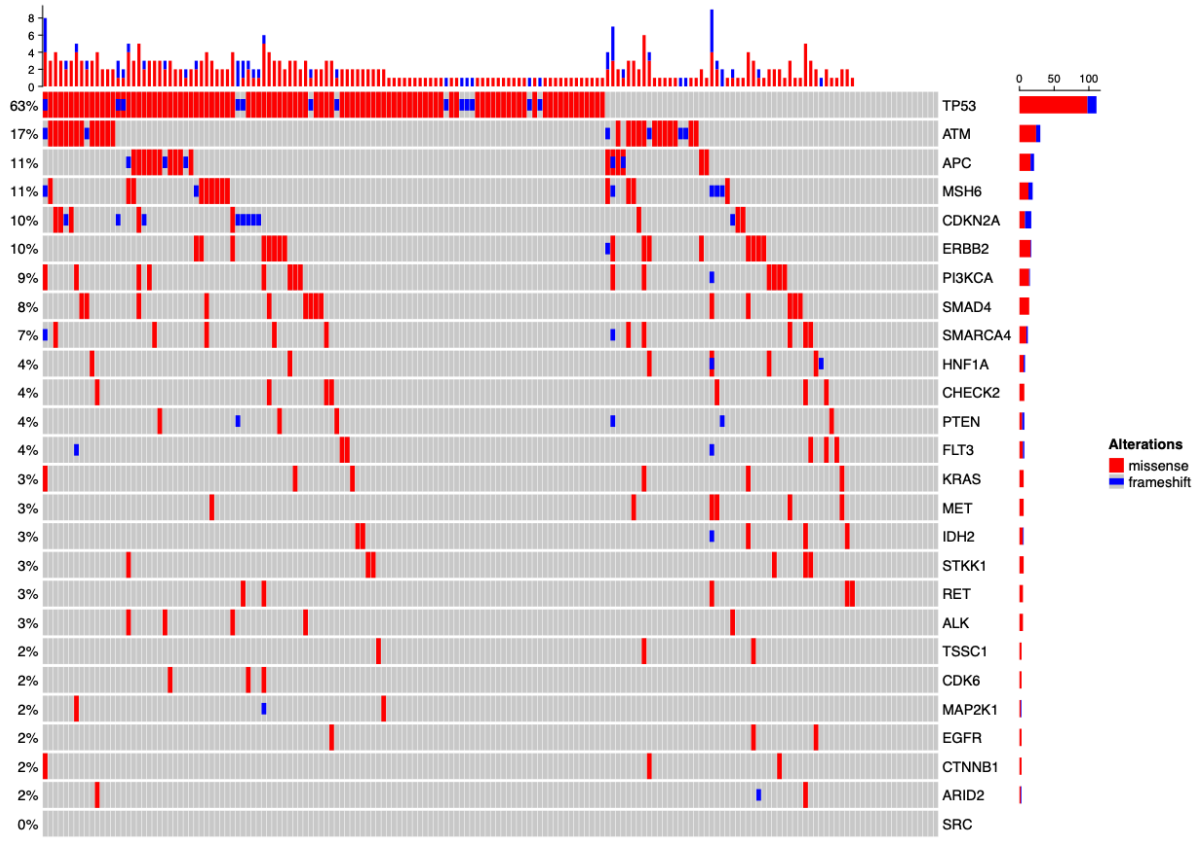

Figure 12: Variants identified the EAC cohort; in red «missense», in blue «frameshift».

The *TP53* gene, which was found mutated in 110/164 cases (67.1%), was the most frequently altered gene. *ATM* (32/164), *APC* (21/164), *MSH6* (19/164), *CDKN2A* (17/164), *PI3KCA* (15/164), *SMAD4* and *ERBB2* (14/164 for each gene) were the other frequently affected genes. There were fewer instances of alteration in other genes.

The majority of the samples (85/164) had multiple, concurrent gene variations, with two samples containing seven or more mutated genes. Only 16 of the 164 samples had no mutations in the 26 cancer-related genes, and 63 samples had just one single mutation in them.

TP53 gene alterations

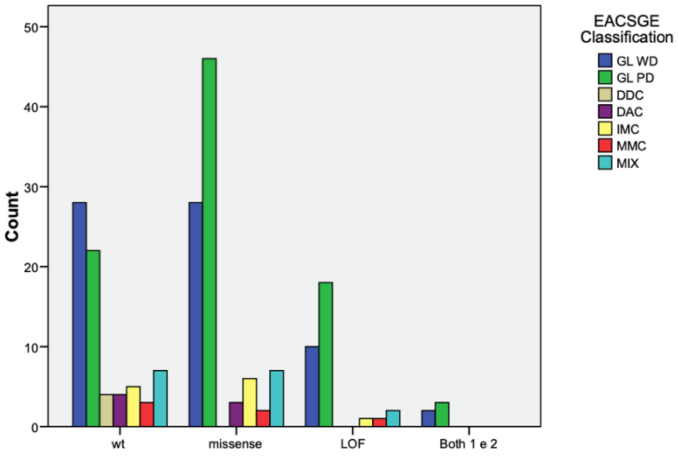

In our EAC cohort, 110 *TP53* variants were identified, and five samples contained multiple *TP53* mutations. Among all *TP53* gene variants, missense and loss-of-function (LOF, including premature stop codon, splice site alterations, and frameshift variants) variants were more prevalent (more than 60 %).

Figure 13: Subtypes of TP53 mutation across our EAC cohort.

Only a few mutations occurred in the Transactivation domain (TAD) or the Proline rich domain (Pro), and only one mutation is localized in the tetramerization domain. The mutations were mostly found in the DNA-binding domain (96/110) of the *TP53* coding region (TD) as showed in Figure 14.

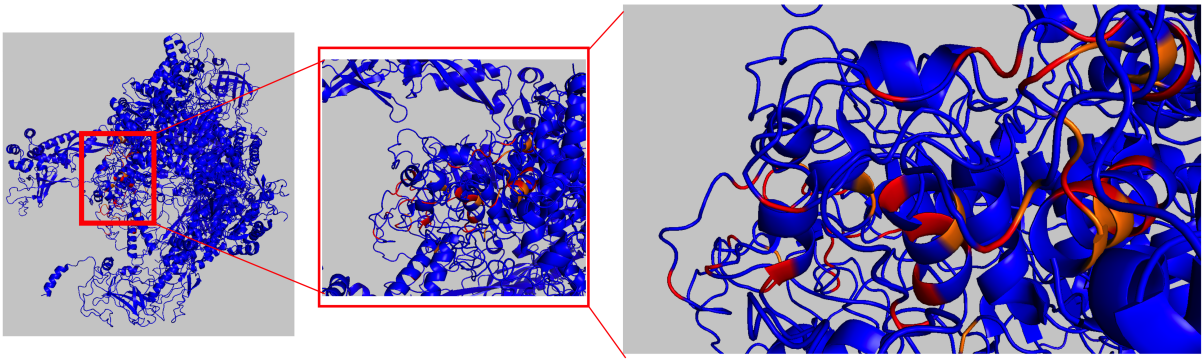

Figure 14: 3D representation of p53 protein. Zooming on DNA binding domain, it's possible to see where the protein is more affected by mutations in our EAC cohort (red) with few hotspots (orange).

Only 2 variants (missense and splice variant) were predicted to tolerate by the "TP53 database" (https://tp53.isb-cgc.org/), and 76 out of 77 missense changes in *TP53* found in our EAC cohort were functionally harmful (98.7%) (Table 3).

Table 3:

TP53	Domain function	Residue function	Effect	exons 11	Damaging	Category based on histology
Chr17: 7574003-G-A | rs730882029	Tetramerisation/NES	NA	nonsense	10	NA	INT PD
Chr17: 7577120-C-T | rs28934576	DNA binding	DNA binding	missense		Damaging	INT WD
Chr17: 7577094-G-A | rs28934574	DNA binding	Buried	missense		Damaging	INT WD
Chr17: 7577104-A-AGGACAGGCACAAACAC	DNA binding	Buried	NA	8	NA	GL PD
Chr17: 7577114-C-A	DNA binding	DNA binding	missense		Damaging	MIX Intest PD/Diff anap
Chr17: 7578176-C-A | COSM118939	NA	NA	splice	intron 6-7	NA	GL PD
Chr17: 7578271-T-A | rs786201838	DNA binding	Buried	missense		Damaging	GL PD
Chr17: 7577539-G-A | rs121912651	DNA binding	DNA binding	missense		Damaging	GL WD
Chr17: 7579463-G-/	SH3-like/Pro-rich	NA	FS	4	NA	INT WD
Chr17: 7577120-C-T | rs28934576	DNA binding	DNA binding	missense		Damaging	INT PD
Chr17: 7577082-C-A | COSM10726	DNA binding	Partially exposed	nonsense	8	NA	GL PD
Chr17: 7577548-C-T | rs28934575	DNA binding	Buried	missense		Damaging	GL WD
Chr17: 7577114-C-T | rs863224451	DNA binding	DNA binding	missense		Damaging	GL PD
Chr17: 7579314-TGCAAGTCACA-T	DNA binding	Buried	NA	4	NA	GL WD
Chr17: 7577586-A-C | COSM10715	DNA binding	Buried	missense		Damaging	GL WD
Chr17: 7577139-G-C	DNA binding	Buried	missense		Damaging	INT PD
Chr17: 7577121-G-A | rs121913343	DNA binding	DNA binding	missense		Damaging	INT WD
Chr17: 7578370-C-A | COSM131534	NA	NA	splice	intron 5-6	NA	GL WD
Chr17: 7577580-T-C | rs587780073	DNA binding	Buried	missense		Damaging	GL PD
Chr17: 7577538-C-T | rs11540652	DNA binding	DNA binding	missense		Damaging	INT WD
Chr17: 7578419-C-A | COSM10996	DNA binding	Partially exposed	nonsense	5	NA	MIX GL PD + DIFF ANAPL
Chr17: 7577538-C-T | rs11540652	DNA binding	DNA binding	missense		Damaging	GL PD
Chr17: 7578212-G-A | rs397516436	DNA binding	Buried	nonsense	6	NA	GL WD
Chr17: 7579346-AAGAAGCCC-A	DNA binding	NA	NA	4	NA	GL PD
Chr17: 7578509-A-G | rs1057519978	DNA binding	S-glutathionylation site	missense		Damaging	GL PD
Chr17: 7578272-G-A | rs876658468	DNA binding	Buried	missense		Damaging	GL PD
Chr17: 7577094-G-A | rs28934574	DNA binding	Buried	missense		Damaging	GL PD
Chr17: 7578380-C-CT	DNA binding	Exposed	missense		Damaging	GL WD
Chr17: 7579326-A-ACTTGGCTG	DNA binding	DNA binding	NA	4	NA	GL PD
Chr17: 7579506-C-CTGGACCTGGGTCTTCAG	SH3-like/Pro-rich	NA	NA	4	NA	GL PD
Chr17: 7577120-C-T | rs28934576	DNA binding	DNA binding	missense		Damaging	INT PD
Chr17: 7577094-G-A | rs28934574	DNA binding	Buried	missense		Damaging	GL PD
Chr17: 7578403-C-A | COSM10645	DNA binding	Zn binding	missense		Damaging	Muc PD
Chr17: 7577539-G-A | rs121912651	DNA binding	DNA binding	missense		Damaging	GL PD
Chr17: 7578463-G-C	DNA binding	Partially exposed	missense		Tolerated	GL PD
Chr17: 7577539-G-A | rs121912651	DNA binding	DNA binding	missense		Damaging	GL PD
Chr17: 7578196-A-C | COSM44198	DNA binding	Buried	missense		Damaging	GL PD
Chr17: 7577539-G-A | rs121912651	DNA binding	DNA binding	missense		Damaging	GL WD
Chr17: 7577094-G-A | rs28934574	DNA binding	Buried	missense		Damaging	GL WD
Chr17: 7578525-G-C | rs1057519976	DNA binding	Buried	missense		Damaging	DIFF ANAPL
Chr17: 7577117-A-G | COSM131453	DNA binding	Buried	missense		Damaging	GL PD
Chr17: 7579560-A-C	Transactivation TAD2	NA	missense		Tolerated	INT WD
Chr17: 7577550-C-T | rs1057517983	DNA binding	Exposed	missense		Damaging	MIX (GL PD + DIFF ANAPL)
Chr17: 7578271-T-C | rs786201838	DNA binding	Buried	missense		Damaging	GL WD
Chr17: 7578269-G-A | rs587780071	DNA binding	Buried	missense		Damaging	GL PD
Chr17: 7577105-G-A | rs876659802	DNA binding	Buried	missense		Damaging	GL WD
Chr17: 7579722-C-T	NA	NA	splice	intron 2-3	NA	GL WD
Chr17: 7578542-G-C | rs863224683	DNA binding	Partially exposed	missense		Damaging	GL WD
Chr17: 7579312-C-A | rs55863639	DNA binding	Buried	splice		Tolerated	GL WD
Chr17: 7577505-T-A	DNA binding	ADP-ribosylation	missense		Damaging	INT WD
Chr17: 7577106-G-A | COSM10814	DNA binding	Buried	missense		Damaging	GL PD
Chr17: 7578431-G-A | COSM11333	DNA binding	Exposed	nonsense	5	NA	INT WD
Chr17: 7577120-C-T | rs28934576	DNA binding	DNA binding	missense		Damaging	GL PD
Chr17: 7579374-C-A	DNA binding	Buried	missense		Damaging	GL PD
Chr17: 7577538-C-T | rs11540652	DNA binding	DNA binding	missense		Damaging	GL WD
Chr17: 7579368-A-C | COSM220765	DNA binding	NA	missense		Damaging	GL PD
Chr17: 7577547-C-T | rs121912656	DNA binding	Buried	missense		Damaging	GL PD
Chr17: 7577539-G-A | rs121912651	DNA binding	DNA binding	missense		Damaging	INT WD
Chr17: 7578406-C-T | rs28934578	DNA binding	Buried	missense		Damaging	INT WD
Chr17: 7578524-G-C | COSM11166	DNA binding	Buried	missense		Damaging	GL PD
Chr17: 7578475-G-A | rs587782705	DNA binding	Partially exposed	missense		Damaging	GL PD
Chr17: 7578212-G-A | rs397516436	DNA binding	Buried	nonsense	6	NA	GL PD
Chr17: 7577120-C-T | rs28934576	DNA binding	DNA binding	missense		Damaging	GL WD
Chr17: 7578197-C-CCACCA	DNA binding	Buried	FS	6	NA	GL PD
Chr17: 7578265-A-G | rs760043106	DNA binding	Buried	missense		Damaging	GL PD
Chr17: 7578555-C-T | rs868137297	NA	NA	splice	intron 4-5	NA	GL WD
Chr17: 7574003-G-A | rs730882029	Tetramerisation/NES	NA	nonsense	10	NA	GL WD
Chr17: 7577156-C-T | COSM127199	NA	NA	splice	intron 7-8	NA	GL WD
Chr17: 7578406-C-T | rs28934578	DNA binding	Buried	missense		Damaging	MUC PD
Chr17: 7579329-T-C | rs121912658	DNA binding	Acetylation/Ubiquitination site	missense		Damaging	MUC PD
Chr17: 7578403-C-A | COSM10645	DNA binding	Zn binding	missense		Damaging	GL PD
Chr17: 7577106-G-T | COSM10814	DNA binding	Buried	missense		Damaging	GL WD
Chr17: 7577081-T-A | rs1057519985	DNA binding	Partially exposed	missense		Damaging	GL WD
Chr17: 7577538-C-T | rs11540652	DNA binding	DNA binding	missense		Damaging	MIX (GL PD + DIFF)
Chr17: 7577539-G-A | rs121912651	DNA binding	DNA binding	missense		Damaging	GL PD
Chr17: 7579471-/-G | rs730882018	SH3-like/Pro-rich	NA	NA	4	NA	INT PD
Chr17: 7578517-G-A | rs750600586	DNA binding	Partially exposed	missense		Damaging	INT PD
Chr17: 7578475-G-A | rs587782705	DNA binding	Partially exposed	missense		Damaging	GL WD
Chr17: 7577121-G-A | rs121913343	DNA binding	DNA binding	missense		Damaging	GL WD
Ch17: 7578460-A-C | COSM1480073	DNA binding	Buried	missense		Damaging	GL PD
Chr17: 7577106-G-A | COSM10814	DNA binding	Buried	missense		Damaging	Muc PD
Chr17: 7578550-G-T | COSM1637542	DNA binding	Buried	missense		Damaging	MUC WD
Chr17: 7577538-C-T | rs11540652	DNA binding	DNA binding	missense		Damaging	GL PD
Chr17: 7578406-C-T | rs28934578	DNA binding	Buried	missense		Damaging	GL PD
Chr17: 7577121-G-A | rs121913343	DNA binding	DNA binding	missense		Damaging	GL PD
Chr17: 7577574-T-C | COSM10731	DNA binding	Buried	missense		Damaging	GL PD
Chr17: 7578452-TG-T | COSM44130	DNA binding	Buried	FS	5	NA	GL PD
Chr17: 7578406-C-T | rs28934578	DNA binding	Buried	missense		Damaging	GL PD

Chr17: 7577538-C-T | rs11540652	DNA binding	DNA binding	missense		Damaging	MUC WD
Chr17: 7578431-G-A | COSM11333	DNA binding	Exposed	nonsense	5	NA	GL PD
Chr17: 7577538-C-T | rs11540652	DNA binding	DNA binding	missense		Damaging	GL WD
Chr17: 7578406-C-T | rs28934578	DNA binding	Buried	missense		Damaging	DIFF ANAPL
Chr17: 7578256-TC-T | COSM118010	DNA binding	Partially exposed	FS	6	NA	GL PD
Chr17: 7578291-T-C | COSM1679503	NA	NA	splice	intron 5-6	NA	GL PD
Chr17: 7577550-C-T | rs1057517983	DNA binding	Exposed	missense		Damaging	GL WD
Chr17: 7578394-T-C | rs1057519991	DNA binding	Zn binding	missense		Damaging	MUC PD
Chr17: 7579311-C-A | COSM127204	NA	NA	splice	intron 4-5	NA	GL WD
Chr17: 7578406-C-T | rs28934578	DNA binding	Buried	missense		Damaging	DIFF ANAPL
Chr17: 7577094-G-A | rs28934574	DNA binding	Buried	missense		Damaging	MUC PD
Chr17: 7577538-C-T | rs11540652	DNA binding	DNA binding	missense		Damaging	GL PD
Chr17: 7577141-C-A | rs193920774	DNA binding	Buried	missense		Damaging	MUC PD
Chr17: 7578403-C-A | COSM10645	DNA binding	Zn binding	missense		Damaging	GL WD
Chr17: 7578279-*-A | COSM1480064	DNA binding	Partially exposed	FS	6	NA	
Chr17: 7577097-C-T | rs764146326	DNA binding	Buried	missense		Damaging	GL PD
Chr17: 7578437-G-A	DNA binding	Partially exposed	nonsense	5	NA	GL PD
Chr17: 7578406-C-T | rs28934578	DNA binding	Buried	missense		Damaging	GL PD
Chr17: 7577121-G-A | rs121913343	DNA binding	DNA binding	missense		Damaging	MIX Intest PD/Diff anap
Chr17: 7577121-G-A | rs121913343	DNA binding	DNA binding	missense		Damaging	GL PD
Chr17: 7578534-C-A | rs866775781	DNA binding	Ubiquitination site	missense		Damaging	MIX (DIFF ANAPL + MUC PD + GL WD)
Chr17: 7578280-G-A | COSM100027	DNA binding	Partially exposed	missense		Damaging	MIX (GL WD + DIFF ANAPL)
Chr17: 7578479-G-C | COSM10905	DNA binding	Buried	missense		Damaging	GL WD
Chr17: 7578263-G-A | rs397516435	DNA binding	Buried	nonsense	6	NA	INT WD
Chr17: 7579865-CTGA-/	Transactivation TAD1/NES	NA	other	2	NA	INT PD
Chr17: 7579454-GCTGGTGCAGGGG-/	SH3-like/Pro-rich	NA	NA	4	NA	INT WD
Chr17: 7579451-G-C	SH3-like/Pro-rich	NA	missense		Tolerated	INT WD
Chr17: 7577599-CAG-C | COSM46164	DNA binding	Exposed	FS	7	NA	GL PD
Chr17: 7577511-A-AGT	DNA binding	Buried	NA	7	NA	GL PD
Chr17: 7577517-A-T | rs876659675	DNA binding	ADP-ribosylation site	missense		Damaging	GL PD
Chr17: 7578263-G-A | rs397516435	DNA binding	Buried	nonsense	6	NA	MIX (GL PD + DIFF ANAPL)
Chr17: 7578190-T-C | rs121912666	DNA binding	Buried	missense		Damaging	INT WD
Chr17: 7577539-G-A | rs121912651	DNA binding	DNA binding	missense		Damaging	GL PD
Chr17: 7578212-GA-A | rs864309495	DNA binding	Buried	FS	6	NA	GL PD
Chr17: 7578433-G-C | COSM11508	DNA binding	Exposed	nonsense	5	NA	GL WD
Chr17: 7577539-G-A | rs121912651	DNA binding	DNA binding	missense		Damaging	GL PD
Chr17: 7579532-T-TG	Transactivation TAD2	NA	NA	4	NA	GL WD
Chr17: 7578202-A-C | COSM119678	DNA binding	Buried	missense		Damaging	GL WD
Chr17: 7579591-C-T | COSM1610880	NA	NA	splice	intron 3-4	NA	MUC PD
Chr17: 7578211-C-T | rs587778720	DNA binding	Buried	missense		Damaging	GL PD
Chr17: 7578508-C-T | rs587781288	DNA binding	S-glutathionylation site	missense		Damaging	GL PD
Chr17: 7578406-C-T | rs28934578	DNA binding	Buried	missense		Damaging	GL PD
Chr17: 7579470-CG-C | COSM1268331	SH3-like/Pro-rich	NA	FS	4	NA	GL PD
Chr17: 7577538-C-T | rs11540652	DNA binding	DNA binding	missense		Damaging	MIX GL PD + DIFF ANAPL
Chr17: 7579532-T-TG	Transactivation TAD2	NA	NA	4	NA	MUC WD
Chr17: 7579349-A-C | COSM10717	DNA binding	Buried	missense		Damaging	GL PD
Chr17: 7578217-G-A | COSM1386676	DNA binding	Phosphorylation site	missense		Damaging	GL PD
Chr17: 7578526-C-A | COSM10647	DNA binding	Buried	missense		Damaging	GL PD
Chr17: 7578290-C-G | COSM127200	NA	NA	splice	intron 5-6	NA	GL WD
Chr17: 7578406-C-T | rs28934578	DNA binding	Buried	missense		Damaging	INT WD
Chr17: 7578406-C-T | rs28934578	DNA binding	Buried	missense		Damaging	INT PD
Chr17: 7577031-T-/	NA	NA	FS	8	NA	
Chr17: 7577121-G-A | rs121913343	DNA binding	DNA binding	missense		Damaging	INT WD

We calculated the clinical outcomes in relation to the presence of *TP53* variants and to the particular *TP53* variant types, such as missense or LOF variants. Cancer-specific survival (CSS), in particular a poor survival, and recurrence were significantly associated to *TP53* mutations (Chi square test *P*=0.039 and *P*=0.031, Table 4A and B respectively).

Table 4:

A

			CSS		
			0	1	Total
***TP53* mutations**	wild-type	Count (%)	42 (40.4)	17 (28.3)	59
	missense	Count (%)	38 (36.5)	35 (58.3)	73
	LOF	Count (%)	21 (20.2)	8 (13.3)	29
	missense+LOF	Count (%)	3 (2.9%)	0	3
	Total		104	60	164
Pearson's Chi-square=8.340			***P*=0.039**		

B

			Recurrence		
			0	1	Total
***TP53* mutations**	wild-type	Count (%)	37 (39.8)	22 (31)	59
	missense	Count (%)	33 (35.5)	40 (56.3)	73
	LOF	Count (%)	20 (21.5)	9 (12.7)	29
	missense+LOF	Count (%)	3 (3.2)	0	3
	Total		93	71	164
Pearson's Chi-square=8.866			***P*=0.031**		

To evaluate whether *TP53* gene genetic variants correlated with clinical and morpho-functional characteristics, we categorized our cohort of samples according to the EACSGE classification, recently introduced by Fiocca et al [60]. The most representative subgroups of the mutated samples (missense, loss-of-function, LOF, and both) were the glandular PD and WD, as shown by the spectrum of mutations, wherein GL PD there are 1.5 times more missense mutations than in GL WD, as shown in Figure 15.

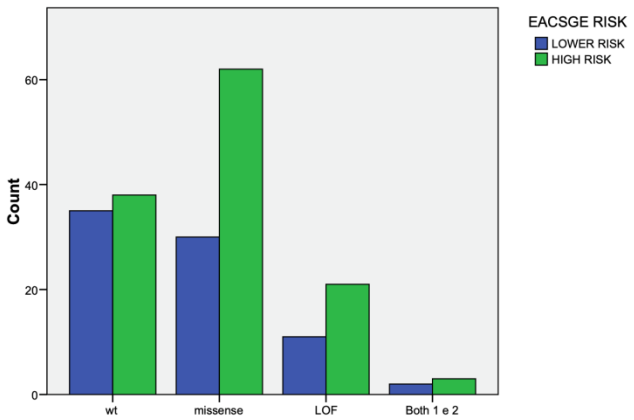

Figure 15: Subtypes of *TP53* variants in EACSGE groups.

Considering the EACGSE classification in Lower Risk and Higher Risk, the presence of *TP53* mutations and the Higher Risk group were significantly associated (Chi square test *P*=0.022, Table 5).

Table 5:

			EACGSE risk		
			Lower risk	Higher risk	Total
***TP53* mutations**	No	Count (%)	28 (47.5)	31 (52.5)	59
	Yes	Count (%)	31 (52.5.5)	74 (70.5)	105
	Total		59	105	164
Pearson's Chi-square=5.275		***P*=0.022**			

These findings led us to expand the scope of the analysis to 202 individuals, including additional EAC cases for which we had genetic material, information on *TP53* mutation status, clinical parameters, and EACGSE-based morphological classification. We could demonstrate that the presence of missense mutations in the Higher Risk cases had a detrimental effect on cancer-specific survival (Long-Rank *P*=0.001 Figure 16A).

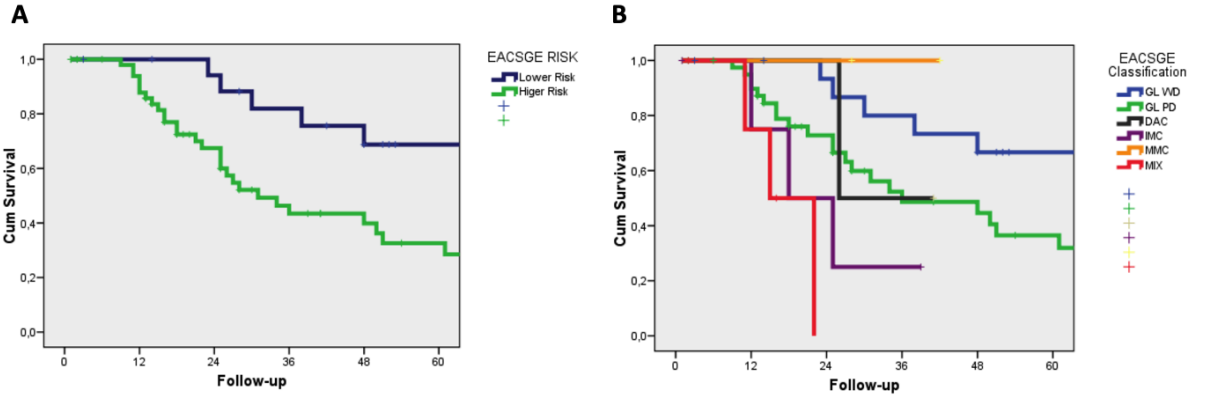

Figure 16: Cancer-specific survival of EAC cases with *TP53* missense variants and p53 expression profiles. (A) Data shown according to Higher and Lower Risk groups. (B) Data shown for the EACSGE morphological subgroups.

When we looked at the various subclasses of the Higher and Lower Risk, we could see that the GD-PD classes were primarily responsible for the statistical association in the presence of the missense variants in the *TP53* gene (Log Rank *P*=1013; Figure 16B).

We considered whether immune-histochemical examination of the tumor specimens could reveal the presence of the various *TP53* variants (missense and LOF). According to our previously described procedures [97], we assessed the presence of various variant types and the staining pattern seen for p53 in terms of overexpression or loss of staining.

For both missense and LOF variants compared to cases without *TP53* variants, there was a significant correlation between the type of mutations and patterns of p53 staining (Spearman correlation coefficient=0.782; $P<0.01$; Figure 17).

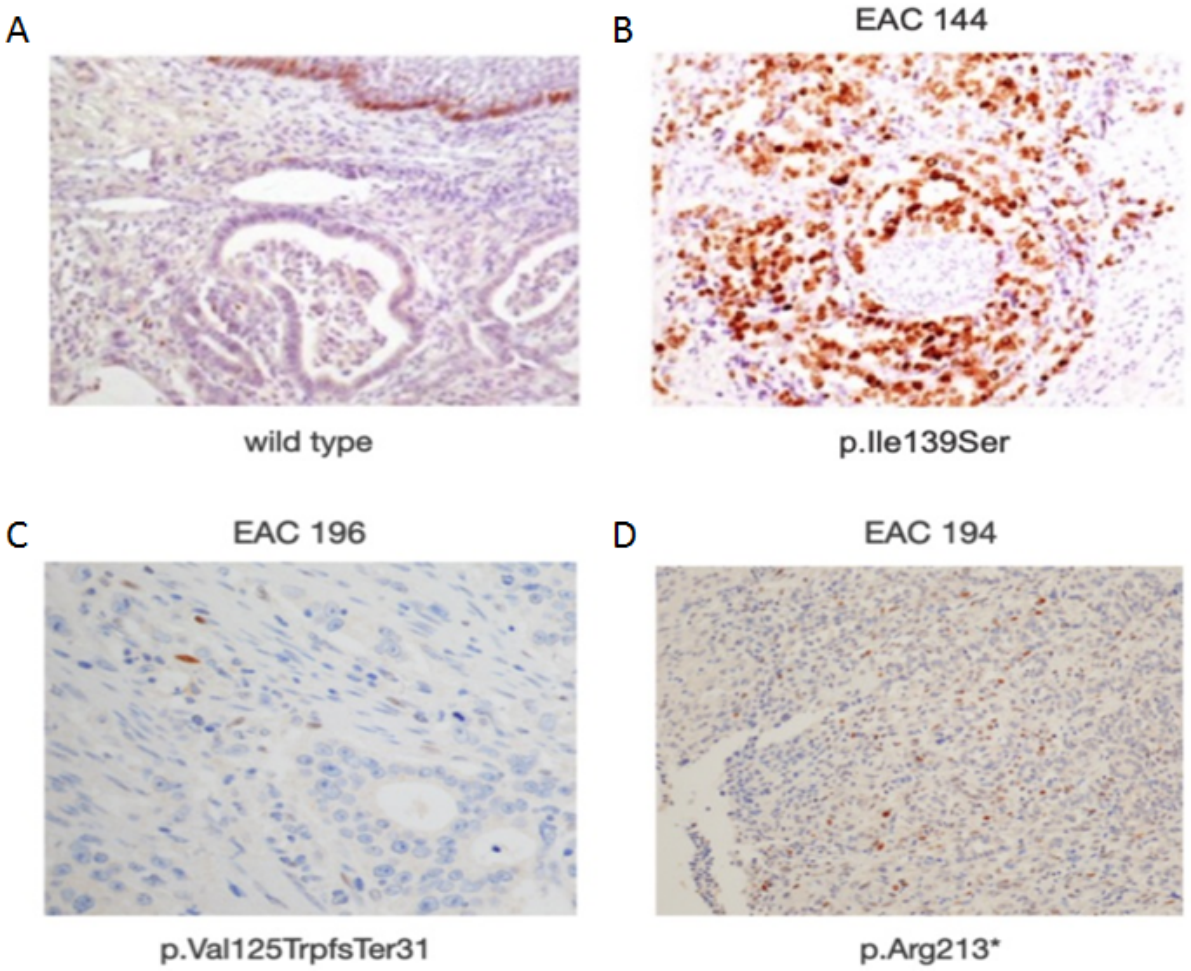

Figure 17: IHC of p53 in (A) control, (B) missense variant, (C-D) LOF variants.

HNF1alpha gene mutations

It is interesting to note that the tumor suppressor gene *HNF1alpha*, which we previously discovered to be mutated in a small number of EAC cases [97], has seven variants in 7 cases (Table 4). In six of seven cases, the *HNF1alpha* gene was mutated alongside other genes such as *TP53*, *PI3KCA*, or *ERBB2*.

The DNA binding domain (three point mutations and one frameshift) and the Transactivation domain were the most heavily mutated regions (2 point mutations and one frameshift).

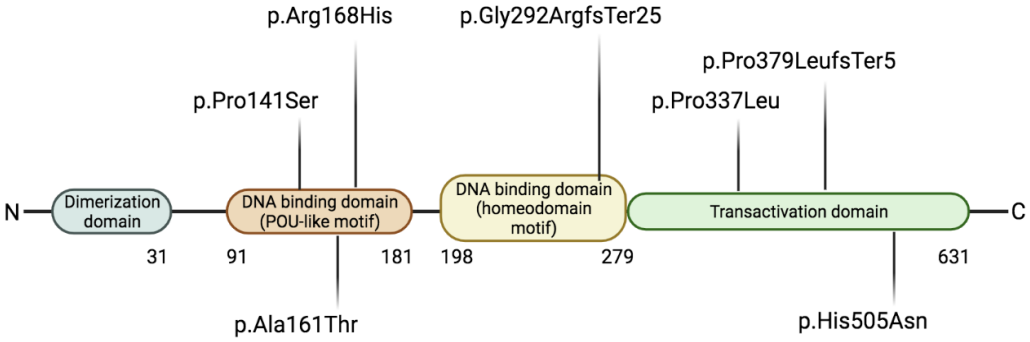

Figure 18: Schematic representation of HNF1alpha gene mutations found in our EAC cohort.

Using the online tool MCAP (MCAP score >0.7; http://bejerano.stanford.edu/mcap/), the missense variants were predicted to be deleterious [103].

We compared the protein expression profiles of the samples with the various *HNF1alpha* variants to a case without mutations (control) using IHC (Figure 19). Patients with *HNF1alpha* damaging variants showed less staining when compared to the control sample. By analyzing NGS data, it was discovered that the decrease in staining was associated with an increase in the frequency of the variant alleles in the tumor (Table 6).

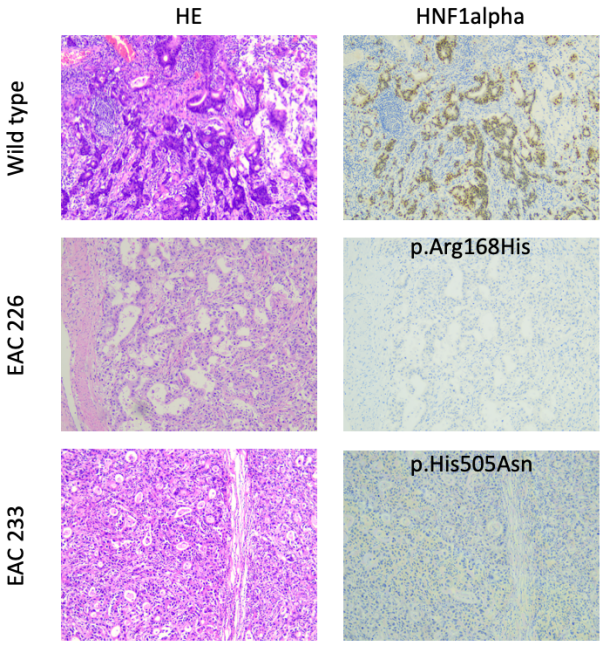

Figure 19: Examples of the immune-histochemical patterns observed in a control sample (i.e., no mutations), *vs*. cases carrying different alterations in *HNF1alpha* gene. In particular, we showed the expression pattern in two cases with the *HNF1alpha* p.Arg168His variant or the p.His505Asn: the decreased staining suggested that the misfolded proteins might be degraded.

Table 6

EAC ID	HNF1alpha variations	gnomAD or COSMIC database	Other genes mutated	HNF1A-IHC 1+ %	HNF1A-IHC 2+ %
150	p.Gly292ArgfsTer25	rs751449138	none	50	50
191	p.Pro337Leu	rs56031130	ATM, TP53,	30	0
192	p.Ala161Thr	rs201095611	PIK3CA	2	0
203	p.Ala161Thr	rs201095611	TP53, PIK3CA	15	0
204	p.Pro141Ser / p.Pro379LeufsTer5	rs150513055 / COSM2175480	SMAD4, IDH2, RET, CTNNB1, FLT3, MET, MSH6, PIK3CA	80	0
226	p.Arg168His	rs377110124	ATM, ERBB2, CTNNB1	2	0
233	p.His505Asn	rs577078110	EGFR	10	0
15	wt			50	0

Twenty-two samples with RNA quality compatible with massive parallel sequencing were sequenced for 1385 oncology-relevant genes at high coverage. Four independent programmes, including FusionCatcher, STAR-Fusion, RNA-Seq Alignment v.1.1.0, and TopHat Alignment v.1.0.0, were used to analyze the data. Only the gene fusions that were discovered in at least three different programs were kept. Nine gene fusions were found in six different EAC cases (Table 7), but we could only confirm six gene fusions in four cases (4/22, 18.2%) using an independent method (Sanger sequencing).

Table 7

EAC ID	Gene fusion identified	Chr_1	Break_1	Chr_2	Break_2	EACSGE classification	EACSGE subgroup	*TP53* status	Sanger confirmed
EAC_197	CYP2C19_CYP2C18	10	96541752	10	96493052	GL PD	High grade	p.Asp208Glu	**YES**
	GIPC1_DNAJB1	19	14602467	19	14627858				**YES**
EAC_198	IQCE_DGKB	7	2629740	7	14385016	GL WD	Low grade	p.Ala138Val	**YES**
EAC_199	PI4KA_MAPK1	22	21096516	22	22153417	GL WD	Low grade	wild-type	**YES**
	CYP2C19_CYP2C18	10	96541752	10	96493052				**YES**
EAC_209	FRYL_PI4KA	4	48686680	22	21104293	GL PD	High grade	p.Arg273Leu - pGln192Ter	**YES**
EAC_210	*AC073283.4-EPCAM*	*2*	*47572040*	*2*	*47606092*	*GL PD*	*High grade*	*wild-type*	*NO*
	LOC101927043-EPCAM	*2*	*47572039*	*2*	*47606091*				*NO*
EAC_298	*TPRG1_LPP*	*3*	*188850486*	*3*	*188242453*	*DIFF ANAPL*		*p.Cys135Trp*	*NO*

It is interesting to note that one of the rearrangements in the two cases with two different gene fusions on chromosome 10 was the same CYP2C19-CYP2C18 fusion (Figure 20).

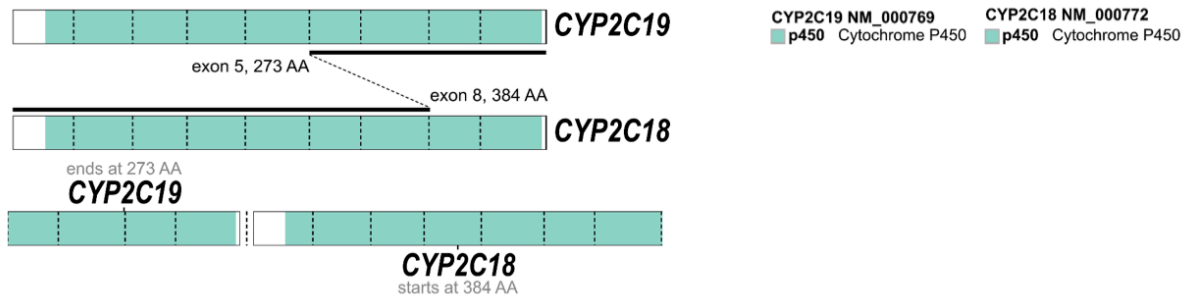

Figure 20: Schematic representation of CYP2C19-CYP2C18 fusion, found in our EAC cohort.

Both genes produce enzymes that belong to the cytochrome P450 superfamily. The cytochrome P450 proteins are monooxygenases that catalyze numerous chemical processes essential for drug metabolism and the production of steroid hormones, cholesterol, and other lipids. The metabolism of retinoids also involves a cytochrome P450 monooxygenase. All trans retinoic acid (atRA) is hydroxylated to 4-hydroxyretinoate, which may influence atRA signaling and clearance [104]. Omeprazole, diazepam, and some barbiturates are among the many xenobiotics that CYP2C19 is known to metabolize [105] whereas the precise substrate of CYP2C18 has not yet been identified.

The GIPC1-DNAJB1 rearrangement was involved in the other gene fusions (Figure 21). A scaffolding protein called GIPC1 (GIPC PDZ Domain Containing Family Member 1) controls the expression and trafficking of cell surface receptors. Oculopharyngodistal Myopathy 2 and Ovary Serous Adenocarcinoma are two conditions linked to GIPC1. G-protein signaling and Syndecan-4-mediated signaling events are two of its related pathways. To promote protein folding and stop misfolded protein aggregation, DNAJB1 encodes for a molecular chaperone that increases the ATPase activity of Hsp70 heat-shock proteins.

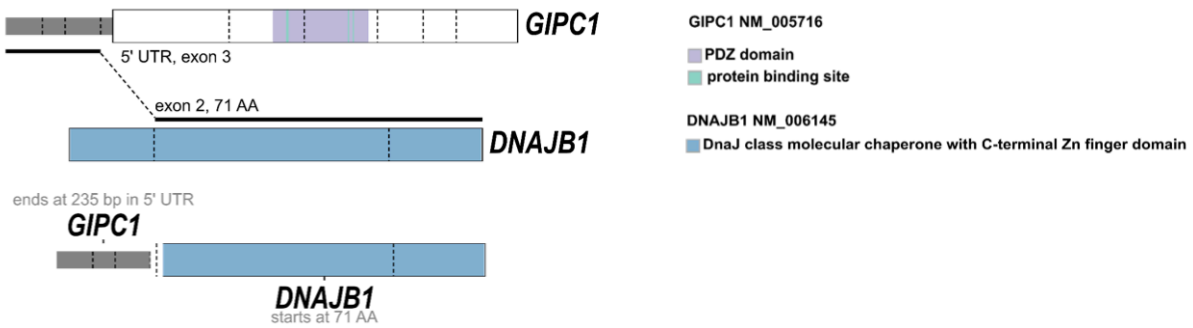

Figure 21: Schematic representation of GIPC1-DNAJB1 fusion, found in our EAC cohort.

Numerous cases of fibrolamellar hepatocellular carcinoma have been found to contain the DNAJB1-PI4KA fusion transcript [106]. Phosphatidylinositol 4-Kinase Alpha (PI4KA) gene was found in two distinct gene fusion EAC samples, one with FYRL and the other with MAPK1 (Figure 22). The first committed step in the biosynthesis of phosphatidylinositol 4,5-bisphosphate is catalyzed by the phosphatidylinositol (PI) 4-kinase that this gene encodes. PI 4-kinases in mammals have been divided into two types, II and III, based on their molecular mass and how detergent and adenosine affect them. By turning on tumor-promoting signals like the RAS pathway, PI4KA is essential in controlling tumorigenesis [107].

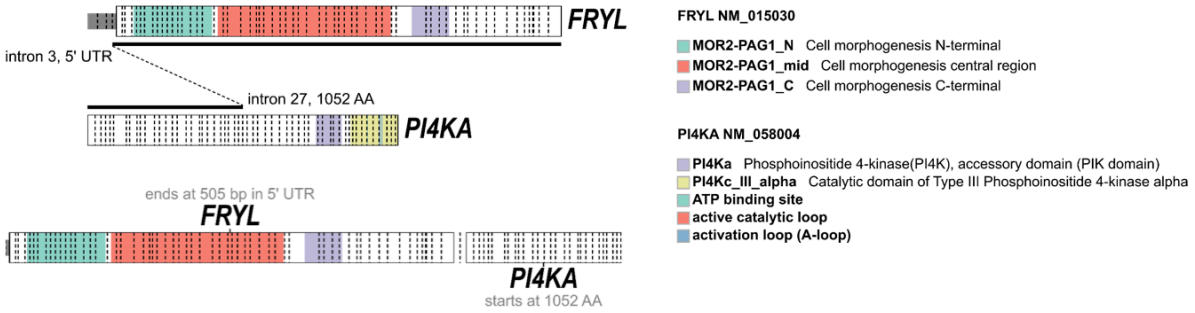

Figure 22: Schematic representation of DNAJB1-PI4KA fusion, found in our EAC cohort.

The fusion of genes IQCE-DGKB (Figure 23) involved the genes for Diacylglycerol Kinase Beta (DGKB), a regulator of the intracellular concentration of the second messenger diacylglycerol (DAG), which plays a crucial role in cellular processes, and IQ Motif Containing E, which is important in limb morphogenesis and also acts as a regulator of Hedgehog signalling [108]. Other gene fusions in prostate cancer have been linked to this latter gene [109].

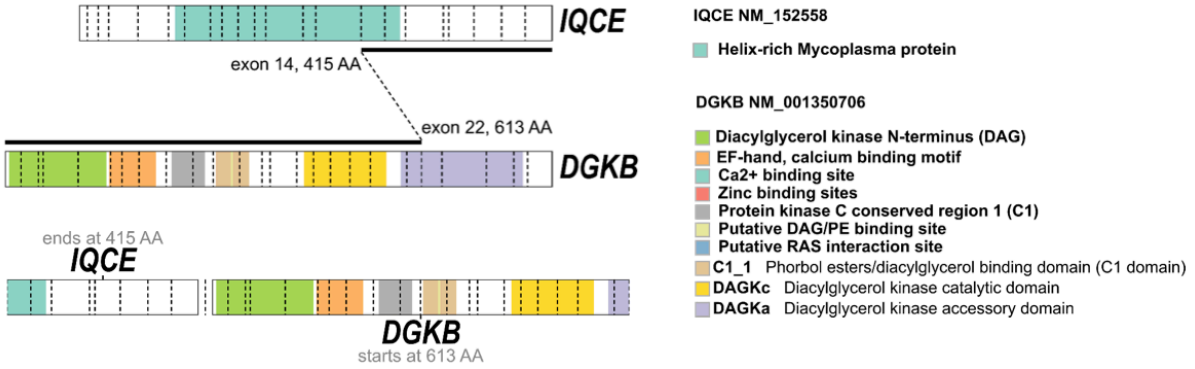

Figure 23: Schematic representation of IQCE-DGKB fusion, found in our EAC cohort.

All the gene fusions involved oncology-related genes, but esophageal adenocarcinoma has not been previously associated to them.

HNF1alpha analysis in EAC cell lines

mRNA analysis of HNF1alpha in cell lines

We used qRT-PCR to assess the expression of *HNF1alpha* in EAC cell lines. In comparison to the other cell lines, the expression level of *HNF1alpha* is significantly higher in OE-19 cell lines (Anova *P*=0.0151). Even when compared to a commercial control, the HNF1alpha expression level in the OE-33 and Flo-1 cell lines was lower (Figure 24).

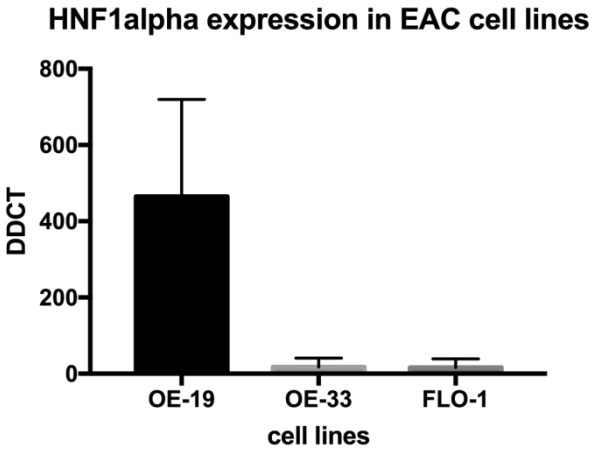

Figure 24: HNF1alpha expression in EAC cell lines

We extracted the DNA from EAC cell lines and used Sanger sequencing to screen the genomic region of the *HNF1alpha* gene to determine the cause of this overexpression. The fact that none of the EAC cell lines had any changes to the coding sequence suggests that HNF1alpha is being overexpressed due to an epigenetic mechanism.

Additionally, as in the 70% of our patients, each EAC cell lines displayed a specific and different *TP53* gene alteration (Figure 25).

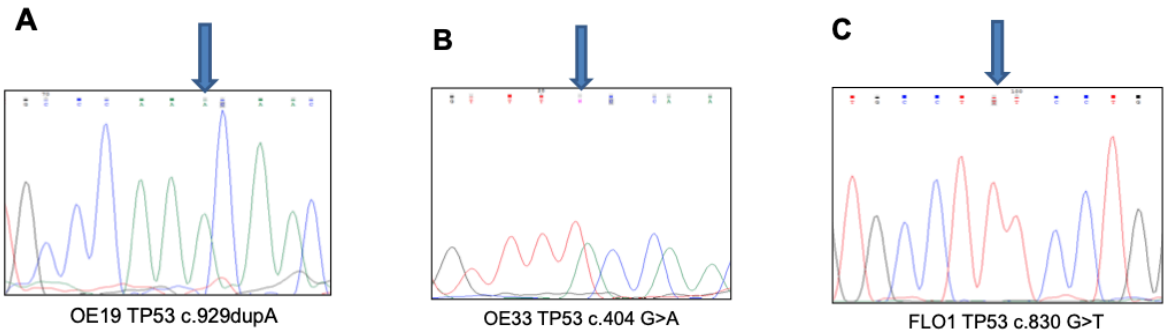

Figure 25: Electropherograms of *TP53* mutations in OE-19, OE-33 and FLO-1 cell lines. (A) The variant c.929dupA is present in OE-19. (B) The variant c.404G>A is present in OE-33 (arrow). (C) The variant c.830G>T is present in FLO-1 (arrow).

We chose to perform HNF1alpha silencing analysis on OE-19 cell lines considering our findings to investigate its possible role as tumor suppressor gene also in EAC.

Fluorescence staining of the mitochondrial network in OE-19 e FLO-1 cell lines

We used MitoTracker Green staining to assess the mitochondrial network in OE-19 and FLO-1 cell lines, since HNF1alpha has not been investigated in esophageal adenocarcinoma. We examined whether the overexpression of HNF1alpha in OE-19 could be the cause of changes in the mitochondrial network, due to its crucial impact for metabolism in various tissues.

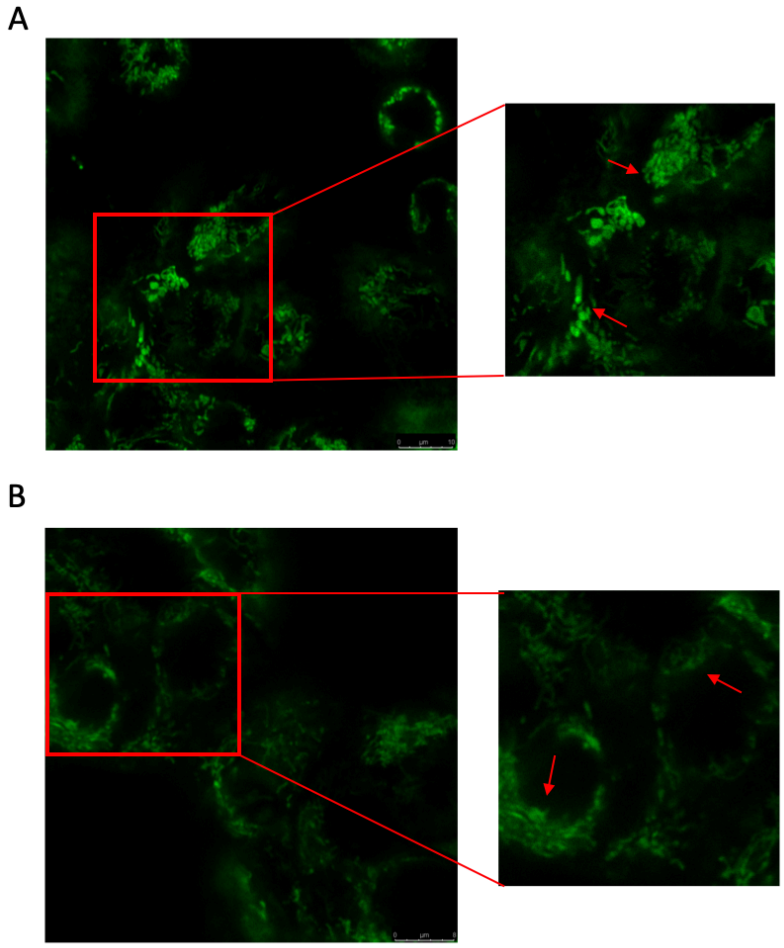

Figure 26: Fluorescence of mitochondrial network of OE-19 (A) and FLO-1 (B) cell lines. Arrows defined mitochondrion localization in the cell.

As shown in Figure 26, both cell lines exhibited a complex network of mitochondria with unstable but erratic connections between each mitochondrion. In terms of organization between the two cell lines, OE-19 cell lines displayed a more aggregated network, whereas FLO-1 cell lines presented a better organization of the mitochondria network (see arrows in Figure 26) in the peripheral area of the cells. We could anyhow infer that each mitochondrial network was specific to a particular cancer cell line, because there was no clear difference between these two cell lines.

Expression level of gDNA and mtDNA of OE-19 and FLO-1 cell lines via qRT-PCR.

To determine whether the overexpression of HNF1alpha results in an increased mitogenesis, we also evaluated the amount of mtDNA in EAC cell lines in comparison to a gDNA. We extracted RNA from both cell lines and used RT-PCR to measure the amount of mtDNA using two crucial mitochondrial genes, ND1 and ND2 [110].

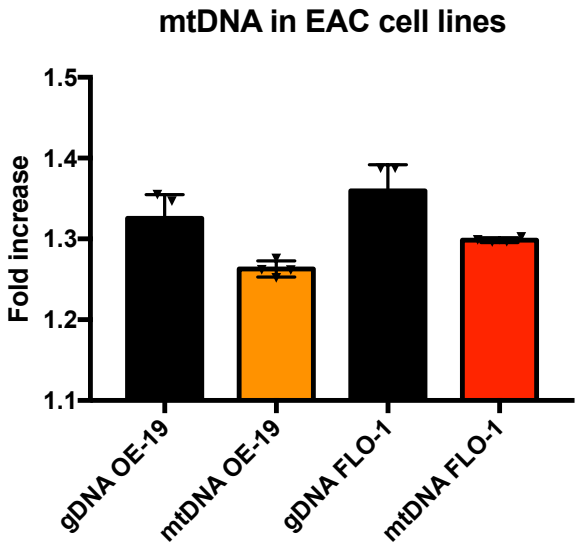

Figure 27: Amount of mtDNA in OE-19 (orange bar) and FLO-1 (red bar) cell lines compared to genomic DNA controls (black bar).

As seen in Figure 27, the amount of mtDNA in both cells is equal to the amount of gDNA. We can draw the conclusion that esophageal adenocarcinoma HNF1alpha overexpression is unrelated to mitogenic processes.

SeaHorse of basal FLO-1 and OE-19 cell lines

The Seahorse XF Analyzers analyze vital cellular processes like glycolysis and mitochondrial respiration by measuring the oxygen consumption rate (OCR) and extracellular acidification rate (ECAR) of live cells in a multi-well plate. OCR is a measure of mitochondrial respiration, and glycolysis primarily contributes to ECAR.

OCR and ECAR are measured in real time by isolating a very tiny volume (roughly 2 µL) of medium above a monolayer of cells in a microplate. The concentrations of dissolved oxygen and free protons in this "transient microchamber" are rapidly, easily measurable changes brought on by cellular oxygen consumption (respiration) and proton excretion (glycolysis), which are measured every few seconds by solid state sensor probes positioned 200 microns

above the cell monolayer. The device measures the concentrations for two to five minutes before computing the OCR and ECAR, respectively.

Following the completion of a measurement, the probes are raised, allowing the larger medium volume above to mix with the medium in the transient microchamber and returning cell values to their initial values. The sequential addition of up to four compounds per well at user-defined intervals is possible with an integrated drug delivery system.

Based on that technology, we initially focused on the basal energetic maps of the FLO-1 and OE-19 cell lines. After making several attempts to determine the best concentration for each cell line, we concluded that the concentration of FCCP for FLO-1 should be around 0.5 M and for OE-19 should be 0.3 M, with an additional input of 0.2 M for both cell lines; the same amount of olygomycin (2 mg/mL) and rotenone/antimycin A (R/A; 1/2 μM) was used.

We observed that FLO-1 cells are significantly more coupled (Figure 28A) and, as a result, generate more energy from the mitochondria.

This is also evident when comparing the OCR/ECAR of FLO-1 cells to OE-19 cells (Figure 28B), which is significantly higher and can significantly increase glycolysis when required. On the other hand OE-19 are cells that are highly dependent on glycolysis since the mitochondria are highly uncoupled (Figure 28A) and it seems that glycolysis cannot be increased if necessary.

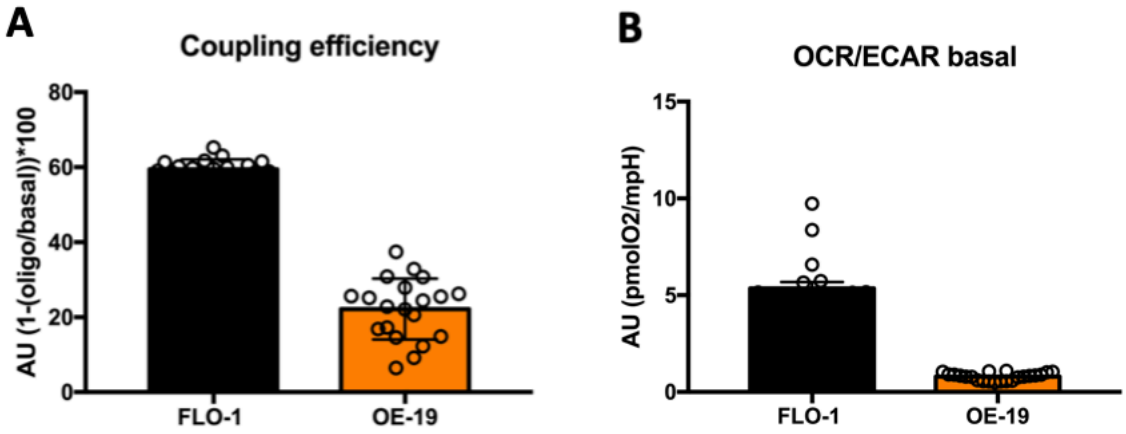

Figure 28: Coupling efficiency (A) and OCR/ECAR basal (B) of FLO-1 and OE-19 cell lines. Oxygen consumption rate (OCR), extracellular acidification rate (ECAR) (OCR/ECAR)

We also observed an intriguing pattern in the cell line responses to oligomycin injection. The antibiotic oligomycin prevents ATP from being produced and from being hydrolyzed when an uncoupler is activated. As shown in Figure 29, when it has been added, it causes the OCR in the cell to decrease. It continues to be stable until FCCP is added, which causes mitochondrial proton permeability.

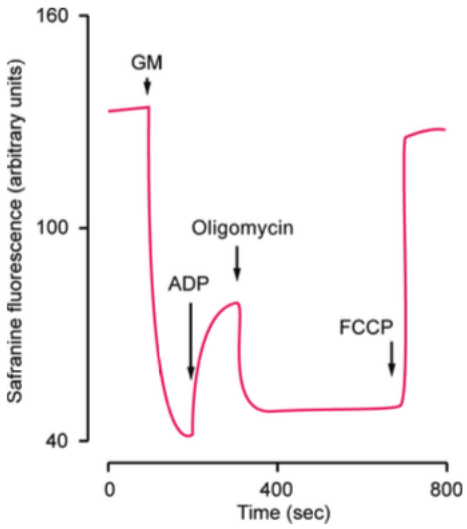

Figure 29: Monitoring Δψ in isolated mitochondria by safranine fluorescence. Brain mitochondria were incubated in the presence of safranine and fluorescence monitored at 495 nm excitation and 585 nm emission. Where indicated, glutamate + malate (GM) ADP, olygomycin and FCCP were added. Note the partial depolarisation going from state 4 to state 3 on addition of ADP. *(From Komary et al. 2010)*

Although this activity is typical for cells, it might not hold true for cancer cells. In fact, Figure 30 clearly demonstrates that OE-19 cell lines do not react the same way. There is only a single initial response when adding 4 mg/mL of olygomycin to OE-19 cells (approximately twice standard used concentration), and even then, the OCR drops slightly.

However, in subsequent measurements, the OCR tends to return to its baseline level (Figure 30A). For FLO-1 cells, which have a significant decrease in OCR level and consistency across measurements, this trend is not the same. Our suggestion is that the olygomycin could not work on these types of cells or it could be throw it out by some mechanisms of drug resistance. Further studies need to be conducted.

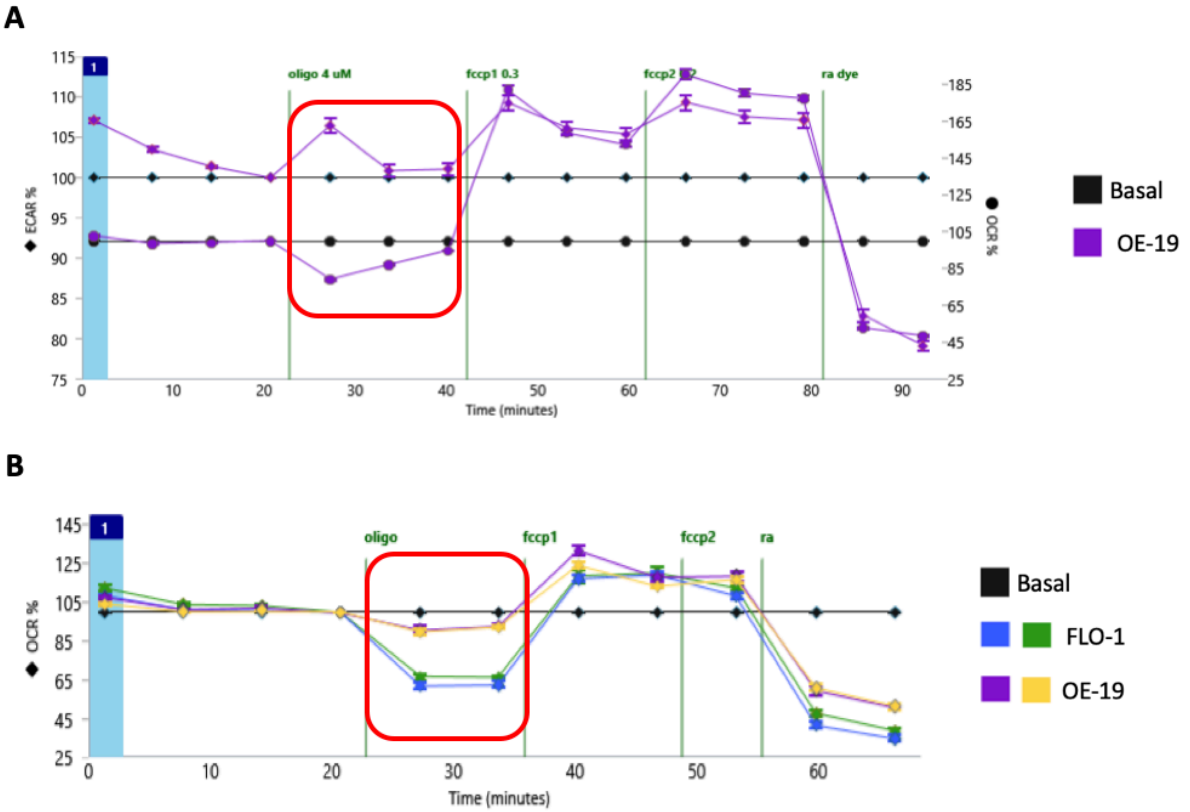

Figure 30: (A) Experiment of OE-19 cells with 4mg/mL of olygomycin. (B) Experiment of comparison between FLO-1 and OE-19 cell based on the response of olygomycin. Red square indicate the measurement of olygomycin in both experiments.

Blocking HNF1alpha by specific siRNA

OE-19 cells were transfected with three different siRNA sequences (siRNA A-B-C) that target HNF1alpha. Three distinct siRNA-mediated HNF1alpha knockdowns resulted in contraposition between them after 96 hours of treatment, according to qRT-PCR analysis.

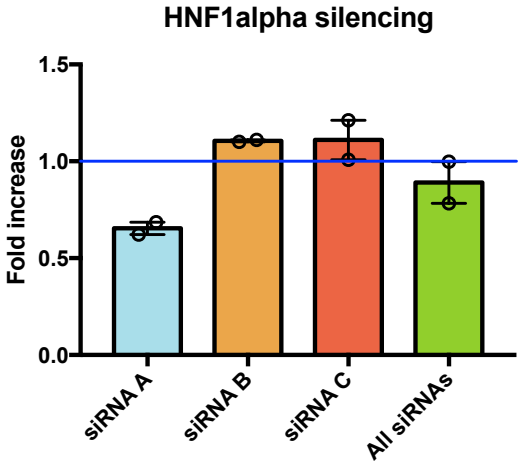

Figure 31: Silencing of HNF1alpha in OE-19 cell lines. Here are represented singular transfection of siRNAs and one transfection with all siRNAs together. Blue line represents basal level of HNF1alpha in OE-19 cell lines

In contrast to siRNA B and siRNA C, which appeared to upregulate HNF1alpha expression in OE-19 cells, only siRNA A showed a reduction in HNF1alpha expression of 40–50% (Figure 31). Due to this, we made the decision to conduct the silencing experiment using only siRNA A.

SeaHorse analysis of HNF1alpha silencing

On OE-19 cells transfected with siRNA A, directs against HNF1alpha mRNA, and the OE-19 cells with only transfection reagent, SeaHorse analysis was performed. We measured the cell's OCR and ECAR as well as the coupling effectiveness of the two cell lines. Figure 32 illustrates that there is no distinction between the siRNA A-transfected cells and the control cells. Figures 32A and 32B show no differences in respiration or oxidation, and Figure 32C shows no differences in coupling efficiency as well as OCR/ECAR measurements (Figure 32D).

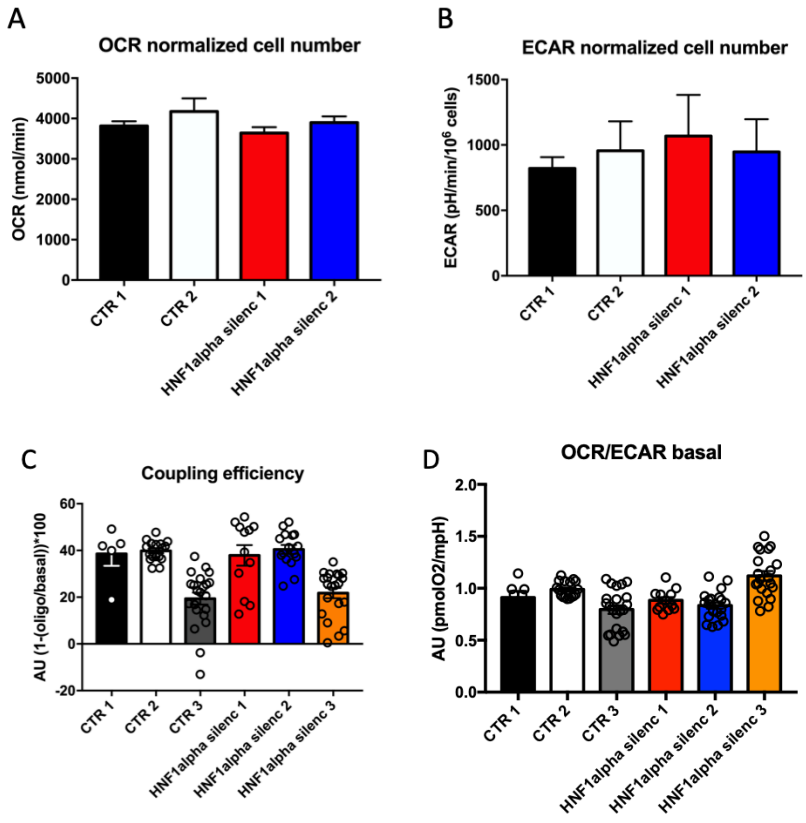

Figure 32: Measurements in OE-19 cell lines with silencing of HNF1alpha compared to control of OCR (A), ECAR (B), coupling efficiency (C) and OCR/ECAR (D).

We also evaluated the expression of HNF1alpha target, GLUT-1, and a tumor proliferation marker, Ki67.

GLUT-1 is a glucose transporter and its expression has been associated with both chemo-resistance and radio-resistance in multiple malignancies [111], [112]. Gastric cancer, ovarian cancer, squamous cell carcinoma, glioblastomas, and meningiomas have been shown to activate GLUT proteins, in particular GLUT-1, GLUT-2, GLUT-3, and GLUT-4. In these tumors, where the Warburg effect is most pronounced, efforts have been made to develop new therapeutic strategies that include preventing the influx of glucose into the tumor cell [113].

Ki67 is a core protein which was expressed in G1, S, G2, and M phase. Its overexpression in breast cancer tumors is associated with a poor prognosis and predicts the effectiveness of neoadjuvant chemotherapy [114]. Along with chemotherapy, the relative proportion of Ki-67 can be seen, and it correlates with the clinical and pathological response in breast cancer [115].

After 72 hours of transient transfection with siRNA A, RNA was extracted and RT-PCR was used to asset the expression of these two targets. With HNF1alpha silenced, no discernible changes were seen in OE-19 cells (Figure 33). Although GLUT-1 expression has slightly decreased, we believe that in order to detect differences, HNF1alpha must be completely silenced.

Figure 33: Expression level of Ki67 and GLUT-1 in OE-19 cell line transfected with siRNA A against HNF1alpha. Blue line represents basal level of targets in OE-19 cells.

Discussion

Due to its rising incidence and poor prognosis, esophageal adenocarcinoma (EAC), which includes cancers of the gastro-esophageal junction, poses a serious health risk in Western nations. Rapid improvements in high-throughput NGS have brought attention to the high EAC heterogeneity both within and between tumors, where many structural genomic rearrangements and mutations can occur even clonally [9], [10] and where epigenetic dysregulation of particular genes can give rise to tumor entities that may behave very differently in terms of progression and resistance [116], [117]. Because of this, there is a growing interest in developing molecular biomarkers for patient stratification and prognosis [24] with the goals of improving existing expression markers, investigating new diagnostic procedures, or creating novel therapeutic targets.

With 8–10 mutations per megabase (mut Mb^{-1}) [118], [119] esophageal adenocarcinoma (EAC) exhibits one of the highest single-base mutational burdens, along with high rates of complex structural variations, deletions, and tandem duplications [116], [120], [121]. Despite the high mutational load, researchers have found few recurrent point mutations in driver genes, with the exception of the tumor suppressor *TP53* (>70% frequency). Other canonical driver genes with recurrent point mutations include *SMAD4* (which encodes a DNA-binding transcription factor and is involved in the TGF pathway), *ARID1A* (which encodes a SWI/SNF chromatin remodelling complex protein), and *CDKN2A* (which encodes the cyclin-dependent kinase inhibitor p16 that regulates p53) recurrently displaying point mutations in less than 20% of cases [10], [122]. In addition to point mutations, patients with EAC also frequently exhibit whole-genome duplication, aneuploidy, frequent CNAs, and aneuploidy as defined in other tissue types [123]. These various molecular characteristics shed light on the disease early development.

EAC has a high burden of structural aberrations and CNAs, according to sequencing studies conducted on hundreds of patients. It has been discovered that loci that contain canonical cancer genes like *ERBB2*, *EGFR*, *GATA4*, *GATA6*, and *RUNX1* are frequently amplified or lost in EAC [10], [122]. Genomic catastrophes like chromothripsis and kataegis are frequent (frequency 30%), and there is evidence that extrachromosomal DNA, focal amplifications, and breakage-fusion-bridge processes are what are responsible for the high CNA rates [124].

Previous biomarker studies have examined gene methylation, copy number/aneuploidy, mutations, and chromosomal alterations in an effort to improve patient stratification [125]. In our study, we concentrated on a set of cancer-related genes that had previously been identified as being mutated repeatedly in a small cohort of EAC cases [97]. TP53 was the most frequently mutated gene, according to previous studies conducted by The Cancer Genome Atlas (TCGA) Research Network [9] and others [126]. 164 EAC samples displayed different patterns of mutations due to the high degree of genetic heterogeneity.

We compared the effects of different mutations (missense changes vs. loss-of-function) in relation to histological and clinical data, and we found that the presence of harmful missense variants in *TP53* adversely affected cancer-specific survival in cases classified as "higher risk" according to the EACGSE classification. Therefore, early detection of *TP53* mutations should be crucial, especially from the standpoint of choosing the most effective strategy for target therapies. Tumor *TP53* mutation was, in fact, the most compelling evidence discovered for an outcome marker. Similar findings have been reported in breast and colorectal carcinoma and Findlay at el. discovered that *TP53* mutant tumors are less chemo(radio)sensitive [127], [128].

Exons 5–9, which encode the DNA binding domain, contain approximately the 95% of functional mutations, and these mutations typically result in loss of efficacy either directly through disruption of DNA contact or indirectly through abnormal protein folding [129]. Cell cycle, DNA repair, and apoptosis regulation may subsequently fail [130], although oncogenic gains of function are occasionally seen [131].

There has been active research into the potential value of p53 IHC as a biomarker of Barrett's progression to adenocarcinoma. Despite the fact that many of these studies had promising results, their shortcomings prevented their widespread adoption [36]. When discussing p53 as an esophageal tumor biomarker, TP53 status (aberrant expression, with or without mutation) is frequently used. A meta-analysis for SCC has shown a correlation between expression alone and a worse outcome. However, there may be a discrepancy between TP53 mutational and expression statuses [132], especially when high-impact mutations prevent expression or sharply shorten half-life. Given that this can be predicted using sequencing data, it is even more important to investigate how these aspects of status interact with one another simultaneously [133], [134].

Resection samples are typically used to analyze relationships between tumor markers and the pathological outcome of chemotherapy. These, however, are clonal populations chosen for chemo- and radio-resistance by definition. The true pre-treatment predictive value of *TP53* mutations in this regard must be established, even though such tumors appear to be disproportionately *TP53* mutated. This will require deep re-sequencing and clonal studies comparing the prevalence and associations of pre- and post-treatment tumor. Targeting mutant p53 is likewise a promising tactic, and various methods are currently being developed to reactivate p53 activity. In the presence of missense mutations, some substances, such as PRIMA-1met APR-246, can restore the activity of mutant p53 [135].

Intriguingly, using a high throughput RNA sequencing method, we discovered a number of gene fusion transcripts (18.2%) involving genes related to oncology. Although there was no obvious statistical correlation between the samples' single nucleotide variants or histological features, also due to the small number of analyzed cases, the discovered gene fusions in EAC have the potential to be important for tumor development and progression. We propose that this analysis would add another step toward comprehending the molecular complex nature of EAC, in line with other studies looking at the structural rearrangements in EAC [136], even though the number of cases for which RNA was available was too small to draw statistically significant conclusions.

In seven cases, we discovered variants in the *HNF1alpha* gene, which we had previously discovered to be mutated in a small number of EAC cases [97]. HNF1alpha is a transcriptional factor that controls the transition from epithelial to mesenchymal tissue and is regarded as a tumor suppressor in pancreatic cancer [94]. It plays a significant role in liver cancers and cell stemness with implications for metabolism. Numerous clinical and laboratory studies came to the conclusion that downregulation of HNF-1alpha was associated with the development of liver tumors that continue to have metabolic dysregulations. The precise mechanism by which HNF-1alpha operates is still unknown, but to date, HNF-1alpha regulations have listed GLUT-1 TNF- α, SHP-1, CDH17, SIRT, and MIA-2.

In this study, we have provided some experimental support for the hypothesis that the pancreatic cancer tumor suppressor gene HNF1alpha may function. First, we evaluated the IHC of patients with HNF1alpha altered and, as expected, a correlation between level of HNF1alpha and variations has been found. Secondly, we focused on energetic/mitochondria aspects. The mRNA levels of reduced HNF1alpha expression in human

esophageal adenocarcinoma were found. In the second step of HNF1alpha silencing, we used SeaHorse analysis to measure metabolism but we found no variation in respiration (OCR), glycolysis (ECAR) or level of HNF1alpha target as GLUT-1, suggesting that HNF1alpha silencing should be done at genomic level (as CRISPR-Cas9 genome editing technique) to better determine its action in tumor progression and metabolism.

Conclusion

Along with lung and melanoma, EAC is among the top three cancers with the highest mutational burden [120], [121], but it also exhibits a low rate of recurrent mutations in particular genes across patients. Rather, this condition is characterized by high rates of chromosomal instability caused by whole-genome duplications, copy number gains, and losses, as well as other complex structural variation events [10], [122]. Because recent analyses of pan-cancer data sets suggest that a high mutational burden is associated with poor survival across cancer types [137], the high mutational burden in EAC likely contributes to the overall poor 5-year survival of 15% [43], [138].

This is also related to the lack of targeted therapies [43] and the heterogeneity of tumors and patients, which results in a subpar response to standard chemotherapy treatments [139], with only 20% of patients showing a response in EAC. The search for novel therapeutics and the identification of disease molecular subtypes that could enable individualized treatment are both made more difficult by the mutational and patient heterogeneity. First and foremost, TP53 and HNF1alpha may be useful biomarkers for early diagnosis, improved patient characterization, and high-quality treatment monitoring.

References

[1] M. R. Kheyrandish, S. M. Mir, and M. Sheikh Arabi, ‘DNA repair pathways as a novel therapeutic strategy in esophageal cancer: A review study’, *Cancer Rep.*, Sep. 2022, doi: 10.1002/cnr2.1716.

[2] D. J. Uhlenhopp, E. O. Then, T. Sunkara, and V. Gaduputi, ‘Epidemiology of esophageal cancer: update in global trends, etiology and risk factors’, *Clin. J. Gastroenterol.*, vol. 13, no. 6, pp. 1010–1021, Dec. 2020, doi: 10.1007/s12328-020-01237-x.

[3] Y. Zhang, ‘Epidemiology of esophageal cancer’, *World J. Gastroenterol.*, vol. 19, no. 34, p. 5598, 2013, doi: 10.3748/wjg.v19.i34.5598.

[4] A. P. Thrift and D. C. Whiteman, ‘The incidence of esophageal adenocarcinoma continues to rise: analysis of period and birth cohort effects on recent trends’, *Ann. Oncol.*, vol. 23, no. 12, pp. 3155–3162, Dec. 2012, doi: 10.1093/annonc/mds181.

[5] A. Ruffato *et al.*, ‘Esophagogastric Metaplasia Relates to Nodal Metastases in Adenocarcinoma of Esophagus and Cardia’, *Ann. Thorac. Surg.*, vol. 95, no. 4, pp. 1147–1153, Apr. 2013, doi: 10.1016/j.athoracsur.2012.12.040.

[6] B. P. L. Wijnhoven, H. W. Tilanus, and W. N. M. Dinjens, ‘Molecular Biology of Barrett’s Adenocarcinoma:’, *Ann. Surg.*, vol. 233, no. 3, pp. 322–337, Mar. 2001, doi: 10.1097/00000658-200103000-00005.

[7] I. Kalatskaya, ‘Overview of major molecular alterations during progression from Barrett’s esophagus to esophageal adenocarcinoma’, *Ann. N. Y. Acad. Sci.*, vol. 1381, no. 1, pp. 74–91, Oct. 2016, doi: 10.1111/nyas.13134.

[8] A. M. Dulak *et al.*, ‘Exome and whole-genome sequencing of esophageal adenocarcinoma identifies recurrent driver events and mutational complexity’, *Nat. Genet.*, vol. 45, no. 5, pp. 478–486, May 2013, doi: 10.1038/ng.2591.

[9] The Cancer Genome Atlas Research Network, ‘Integrated genomic characterization of oesophageal carcinoma’, *Nature*, vol. 541, no. 7636, pp. 169–175, Jan. 2017, doi: 10.1038/nature20805.

[10] M. Secrier *et al.*, ‘Mutational signatures in esophageal adenocarcinoma define etiologically distinct subgroups with therapeutic relevance’, *Nat. Genet.*, vol. 48, no. 10, pp. 1131–1141, Oct. 2016, doi: 10.1038/ng.3659.

[11] R. F. Souza, K. Krishnan, and S. J. Spechler, ‘Acid, bile, and CDX: the ABCs of making Barrett’s metaplasia’, *Am. J. Physiol. Gastrointest. Liver Physiol.*, vol. 295, no. 2, pp. G211-218, Aug. 2008, doi: 10.1152/ajpgi.90250.2008.

[12] J. H. Rubenstein and J. B. Taylor, ‘Meta-analysis: the association of oesophageal adenocarcinoma with symptoms of gastro-oesophageal reflux’, *Aliment. Pharmacol. Ther.*, vol. 32, no. 10, pp. 1222–1227, Nov. 2010, doi: 10.1111/j.1365-2036.2010.04471.x.

[13] K. S. Nason *et al.*, ‘Gastroesophageal reflux disease symptom severity, proton pump inhibitor use, and esophageal carcinogenesis’, *Arch. Surg. Chic. Ill 1960*, vol. 146, no. 7, pp. 851–858, Jul. 2011, doi: 10.1001/archsurg.2011.174.

[14] M. B. Cook *et al.*, ‘Cigarette smoking and adenocarcinomas of the esophagus and esophagogastric junction: a pooled analysis from the international BEACON consortium’, *J. Natl. Cancer Inst.*, vol. 102, no. 17, pp. 1344–1353, Sep. 2010, doi: 10.1093/jnci/djq289.

[15] N. D. Freedman *et al.*, ‘Alcohol intake and risk of oesophageal adenocarcinoma: a pooled analysis from the BEACON Consortium’, *Gut*, vol. 60, no. 8, pp. 1029–1037, Aug. 2011, doi: 10.1136/gut.2010.233866.

[16] S. Singh *et al.*, ‘Central adiposity is associated with increased risk of esophageal inflammation, metaplasia, and adenocarcinoma: a systematic review and meta-analysis’, *Clin. Gastroenterol. Hepatol. Off. Clin. Pract. J. Am. Gastroenterol. Assoc.*, vol. 11, no. 11, pp. 1399-1412.e7, Nov. 2013, doi: 10.1016/j.cgh.2013.05.009.

[17] M. H. Derakhshan *et al.*, ‘Mechanism of association between BMI and dysfunction of the gastro-oesophageal barrier in patients with normal endoscopy’, *Gut*, vol. 61, no. 3, pp. 337–343, Mar. 2012, doi: 10.1136/gutjnl-2011-300633.

[18] J. E. Pandolfino, H. B. El-Serag, Q. Zhang, N. Shah, S. K. Ghosh, and P. J. Kahrilas, ‘Obesity: a challenge to esophagogastric junction integrity’, *Gastroenterology*, vol. 130, no. 3, pp. 639–649, Mar. 2006, doi: 10.1053/j.gastro.2005.12.016.

[19] J. M. Garcia *et al.*, ‘Circulating inflammatory cytokines and adipokines are associated with increased risk of Barrett’s esophagus: a case-control study’, *Clin. Gastroenterol. Hepatol. Off. Clin. Pract. J. Am. Gastroenterol. Assoc.*, vol. 12, no. 2, pp. 229-238.e3, Feb. 2014, doi: 10.1016/j.cgh.2013.07.038.

[20] B. Lindkvist *et al.*, ‘Metabolic risk factors for esophageal squamous cell carcinoma and adenocarcinoma: a prospective study of 580,000 subjects within the Me-Can project’, *BMC Cancer*, vol. 14, p. 103, Feb. 2014, doi: 10.1186/1471-2407-14-103.

[21] J. H. Rubenstein *et al.*, ‘Associations of diabetes mellitus, insulin, leptin, and ghrelin with gastroesophageal reflux and Barrett’s esophagus’, *Gastroenterology*, vol. 145, no. 6, pp. 1237-1244.e1–5, Dec. 2013, doi: 10.1053/j.gastro.2013.08.052.

[22] C. Duggan, L. Onstad, S. Hardikar, P. L. Blount, B. J. Reid, and T. L. Vaughan, ‘Association between markers of obesity and progression from Barrett’s esophagus to esophageal adenocarcinoma’, *Clin. Gastroenterol. Hepatol. Off. Clin. Pract. J. Am. Gastroenterol. Assoc.*, vol. 11, no. 8, pp. 934–943, Aug. 2013, doi: 10.1016/j.cgh.2013.02.017.

[23] K. B. Greer *et al.*, ‘Association of insulin and insulin-like growth factors with Barrett’s oesophagus’, *Gut*, vol. 61, no. 5, pp. 665–672, May 2012, doi: 10.1136/gutjnl-2011-300641.

[24] A. R. McElholm *et al.*, ‘A population-based study of IGF axis polymorphisms and the esophageal inflammation, metaplasia, adenocarcinoma sequence’, *Gastroenterology*, vol. 139, no. 1, pp. 204-212.e3, Jul. 2010, doi: 10.1053/j.gastro.2010.04.014.

[25] S. H. Siahpush *et al.*, ‘Longitudinal study of insulin-like growth factor, insulin-like growth factor binding protein-3, and their polymorphisms: risk of neoplastic progression in Barrett’s esophagus’, *Cancer Epidemiol. Biomark. Prev. Publ. Am. Assoc. Cancer Res. Cosponsored Am. Soc. Prev. Oncol.*, vol. 16, no. 11, pp. 2387–2395, Nov. 2007, doi: 10.1158/1055-9965.EPI-06-0986.

[26] F. Islami and F. Kamangar, ‘Helicobacter pylori and esophageal cancer risk: a meta-analysis’, *Cancer Prev. Res. Phila. Pa*, vol. 1, no. 5, pp. 329–338, Oct. 2008, doi: 10.1158/1940-6207.CAPR-08-0109.

[27] D. Y. Graham *et al.*, ‘Challenge model for Helicobacter pylori infection in human volunteers’, *Gut*, vol. 53, no. 9, pp. 1235–1243, Sep. 2004, doi: 10.1136/gut.2003.037499.

[28] A. Raghunath, A. P. S. Hungin, D. Wooff, and S. Childs, ‘Prevalence of Helicobacter pylori in patients with gastro-oesophageal reflux disease: systematic review’, *BMJ*, vol. 326, no. 7392, p. 737, Apr. 2003, doi: 10.1136/bmj.326.7392.737.

[29] J. Luther *et al.*, 'Helicobacter pylori DNA decreases pro-inflammatory cytokine production by dendritic cells and attenuates dextran sodium sulphate-induced colitis', *Gut*, vol. 60, no. 11, pp. 1479–1486, Nov. 2011, doi: 10.1136/gut.2010.220087.

[30] L. M. G. Moons *et al.*, 'A pro-inflammatory genotype predisposes to Barrett's esophagus', *Carcinogenesis*, vol. 29, no. 5, pp. 926–931, May 2008, doi: 10.1093/carcin/bgm241.

[31] Z. Pei, L. Yang, R. M. Peek, S. M. Jr Levine, D. T. Pride, and M. J. Blaser, 'Bacterial biota in reflux esophagitis and Barrett's esophagus', *World J. Gastroenterol.*, vol. 11, no. 46, pp. 7277–7283, Dec. 2005, doi: 10.3748/wjg.v11.i46.7277.

[32] J. B. O'Connor, G. W. Falk, and J. E. Richter, 'The incidence of adenocarcinoma and dysplasia in Barrett's esophagus: report on the Cleveland Clinic Barrett's Esophagus Registry', *Am. J. Gastroenterol.*, vol. 94, no. 8, pp. 2037–2042, Aug. 1999, doi: 10.1111/j.1572-0241.1999.01275.x.

[33] D. J. Drewitz, R. E. Sampliner, and H. S. Garewal, 'The incidence of adenocarcinoma in Barrett's esophagus: a prospective study of 170 patients followed 4.8 years', *Am. J. Gastroenterol.*, vol. 92, no. 2, pp. 212–215, Feb. 1997.

[34] S. J. Spechler, 'Barrett's esophagus and esophageal adenocarcinoma: pathogenesis, diagnosis, and therapy', *Med. Clin. North Am.*, vol. 86, no. 6, pp. 1423–1445, vii, Nov. 2002, doi: 10.1016/s0025-7125(02)00082-2.

[35] M. A. Eloubeidi, R. Desmond, M. R. Arguedas, C. E. Reed, and C. M. Wilcox, 'Prognostic factors for the survival of patients with esophageal carcinoma in the U.S.: the importance of tumor length and lymph node status', *Cancer*, vol. 95, no. 7, pp. 1434–1443, Oct. 2002, doi: 10.1002/cncr.10868.

[36] M. Redston *et al.*, 'Abnormal TP53 Predicts Risk of Progression in Patients With Barrett's Esophagus Regardless of a Diagnosis of Dysplasia', *Gastroenterology*, vol. 162, no. 2, pp. 468–481, Feb. 2022, doi: 10.1053/j.gastro.2021.10.038.

[37] W. L. Curvers *et al.*, 'Low-Grade Dysplasia in Barrett's Esophagus: Overdiagnosed and Underestimated', *Am. J. Gastroenterol.*, vol. 105, no. 7, pp. 1523–1530, Jul. 2010, doi: 10.1038/ajg.2010.171.

[38] On behalf of the International Photodynamic Group for High-Grade Dysplasia in Barrett's Esophagus *et al.*, 'Overdiagnosis of high-grade dysplasia in Barrett's esophagus: a multicenter, international study', *Mod. Pathol.*, vol. 28, no. 6, pp. 758–765, Jun. 2015, doi: 10.1038/modpathol.2015.2.

[39] M. D. Stachler *et al.*, 'Paired exome analysis of Barrett's esophagus and adenocarcinoma', *Nat. Genet.*, vol. 47, no. 9, pp. 1047–1055, Sep. 2015, doi: 10.1038/ng.3343.

[40] S. Killcoyne *et al.*, 'Genomic copy number predicts esophageal cancer years before transformation', *Nat. Med.*, vol. 26, no. 11, pp. 1726–1732, Nov. 2020, doi: 10.1038/s41591-020-1033-y.

[41] Z. Jin *et al.*, 'A multicenter, double-blinded validation study of methylation

biomarkers for progression prediction in Barrett's esophagus', *Cancer Res.*, vol. 69, no. 10, pp. 4112–4115, May 2009, doi: 10.1158/0008-5472.CAN-09-0028.

[42] J. M. J. Weaver *et al.*, 'Ordering of mutations in preinvasive disease stages of esophageal carcinogenesis', *Nat. Genet.*, vol. 46, no. 8, pp. 837–843, Aug. 2014, doi: 10.1038/ng.3013.

[43] E. C. Smyth *et al.*, 'Oesophageal cancer', *Nat. Rev. Dis. Primer*, vol. 3, p. 17048, Jul. 2017, doi: 10.1038/nrdp.2017.48.

[44] M. Younes *et al.*, 'p53 protein accumulation predicts malignant progression in Barrett's metaplasia: a prospective study of 275 patients', *Histopathology*, vol. 71, no. 1, pp. 27–33, Jul. 2017, doi: 10.1111/his.13193.

[45] A. Srivastava, H. Appelman, J. D. Goldsmith, J. M. Davison, J. Hart, and A. M. Krasinskas, 'The Use of Ancillary Stains in the Diagnosis of Barrett Esophagus and Barrett Esophagus-associated Dysplasia: Recommendations From the Rodger C. Haggitt Gastrointestinal Pathology Society', *Am. J. Surg. Pathol.*, vol. 41, no. 5, pp. e8–e21, May 2017, doi: 10.1097/PAS.0000000000000819.

[46] C. Hur *et al.*, 'Trends in esophageal adenocarcinoma incidence and mortality', *Cancer*, vol. 119, no. 6, pp. 1149–1158, Mar. 2013, doi: 10.1002/cncr.27834.

[47] J. H. Rubenstein and N. J. Shaheen, 'Epidemiology, Diagnosis, and Management of Esophageal Adenocarcinoma', *Gastroenterology*, vol. 149, no. 2, pp. 302-317.e1, Aug. 2015, doi: 10.1053/j.gastro.2015.04.053.

[48] W. Januszewicz and R. C. Fitzgerald, 'Barrett's oesophagus and oesophageal adenocarcinoma', *Medicine (Baltimore)*, vol. 47, no. 5, pp. 275–285, May 2019, doi: 10.1016/j.mpmed.2019.02.005.

[49] S. Jain and S. Dhingra, 'Pathology of esophageal cancer and Barrett's esophagus', *Ann. Cardiothorac. Surg.*, vol. 6, no. 2, pp. 99–109, Mar. 2017, doi: 10.21037/acs.2017.03.06.

[50] O. Pech, E. Bollschweiler, H. Manner, J. Leers, C. Ell, and A. H. Hölscher, 'Comparison between endoscopic and surgical resection of mucosal esophageal adenocarcinoma in Barrett's esophagus at two high-volume centers', *Ann. Surg.*, vol. 254, no. 1, pp. 67–72, Jul. 2011, doi: 10.1097/SLA.0b013e31821d4bf6.

[51] U. Ronellenfitsch *et al.*, 'Preoperative chemo(radio)therapy versus primary surgery for gastroesophageal adenocarcinoma: systematic review with meta-analysis combining individual patient and aggregate data', *Eur. J. Cancer Oxf. Engl. 1990*, vol. 49, no. 15, pp. 3149–3158, Oct. 2013, doi: 10.1016/j.ejca.2013.05.029.

[52] J. M. Findlay, M. R. Middleton, and I. Tomlinson, 'A systematic review and meta-analysis of somatic and germline DNA sequence biomarkers of esophageal cancer survival, therapy response and stage', *Ann. Oncol.*, vol. 26, no. 4, pp. 624–644, Apr. 2015, doi: 10.1093/annonc/mdu449.

[53] T. Djärv, M. Derogar, and P. Lagergren, 'Influence of co-morbidity on long-term quality of life after oesophagectomy for cancer', *Br. J. Surg.*, vol. 101, no. 5, pp. 495–501, Apr. 2014, doi: 10.1002/bjs.9417.

[54] V. Gebski *et al.*, 'Survival benefits from neoadjuvant chemoradiotherapy or chemotherapy in oesophageal carcinoma: a meta-analysis', *Lancet Oncol.*, vol. 8, no. 3, pp. 226–234, Mar. 2007, doi: 10.1016/S1470-2045(07)70039-6.

[55] N. P. Campbell and V. M. Villaflor, 'Neoadjuvant treatment of esophageal cancer', *World J. Gastroenterol.*, vol. 16, no. 30, pp. 3793–3803, Aug. 2010, doi: 10.3748/wjg.v16.i30.3793.

[56] Y.-J. Bang *et al.*, 'Trastuzumab in combination with chemotherapy versus chemotherapy alone for treatment of HER2-positive advanced gastric or gastro-oesophageal junction cancer (ToGA): a phase 3, open-label, randomised controlled trial', *Lancet Lond. Engl.*, vol. 376, no. 9742, pp. 687–697, Aug. 2010, doi: 10.1016/S0140-6736(10)61121-X.

[57] D. Kandioler *et al.*, 'The biomarker TP53 divides patients with neoadjuvantly treated esophageal cancer into 2 subgroups with markedly different outcomes. A p53 Research Group study', *J. Thorac. Cardiovasc. Surg.*, vol. 148, no. 5, pp. 2280–2286, Nov. 2014, doi: 10.1016/j.jtcvs.2014.06.079.

[58] F. Amirtharaj *et al.*, 'p53 reactivating small molecule PRIMA-1MET/APR-246 regulates genomic instability in MDA-MB-231 cells', *Oncol. Rep.*, vol. 47, no. 4, p. 85, Apr. 2022, doi: 10.3892/or.2022.8296.

[59] S. Mattioli *et al.*, 'Immunopathological patterns of the stomach in adenocarcinoma of the esophagus, cardia, and gastric antrum: gastric profiles in Siewert type I and II tumors', *Ann. Thorac. Surg.*, vol. 83, no. 5, pp. 1814–1819, May 2007, doi: 10.1016/j.athoracsur.2007.01.016.

[60] R. Fiocca *et al.*, 'The Prognostic Impact of Histology in Esophageal and Esophago-Gastric Junction Adenocarcinoma', *Cancers*, vol. 13, no. 20, p. 5211, Oct. 2021, doi: 10.3390/cancers13205211.

[61] A. R. Davies *et al.*, 'Factors associated with early recurrence and death after esophagectomy for cancer', *J. Surg. Oncol.*, vol. 109, no. 5, pp. 459–464, Apr. 2014, doi: 10.1002/jso.23511.

[62] I. Rouvelas, W. Zeng, M. Lindblad, P. Viklund, W. Ye, and J. Lagergren, 'Survival after surgery for oesophageal cancer: a population-based study', *Lancet Oncol.*, vol. 6, no. 11, pp. 864–870, Nov. 2005, doi: 10.1016/S1470-2045(05)70347-8.

[63] G. Contino, T. L. Vaughan, D. Whiteman, and R. C. Fitzgerald, 'The Evolving Genomic Landscape of Barrett's Esophagus and Esophageal Adenocarcinoma', *Gastroenterology*, vol. 153, no. 3, pp. 657-673.e1, Sep. 2017, doi: 10.1053/j.gastro.2017.07.007.

[64] D. S. Y. Chan, C. P. Twine, and W. G. Lewis, 'Systematic review and meta-analysis of the influence of HER2 expression and amplification in operable oesophageal cancer', *J. Gastrointest. Surg. Off. J. Soc. Surg. Aliment. Tract*, vol. 16, no. 10, pp. 1821–1829, Oct. 2012, doi: 10.1007/s11605-012-1979-2.

[65] N. Agrawal *et al.*, 'Comparative genomic analysis of esophageal adenocarcinoma and squamous cell carcinoma', *Cancer Discov.*, vol. 2, no. 10, pp. 899–905, Oct. 2012, doi: 10.1158/2159-8290.CD-12-0189.

[66] J. N. Patel, H. L. McLeod, and F. Innocenti, ‘Implications of genome-wide association studies in cancer therapeutics’, *Br. J. Clin. Pharmacol.*, vol. 76, no. 3, pp. 370–380, Sep. 2013, doi: 10.1111/bcp.12166.

[67] M. Weller, ‘Predicting response to cancer chemotherapy: the role of p53’, *Cell Tissue Res.*, vol. 292, no. 3, pp. 435–445, Jun. 1998, doi: 10.1007/s004410051072.

[68] A. Petitjean *et al.*, ‘Impact of mutant p53 functional properties on TP53 mutation patterns and tumor phenotype: lessons from recent developments in the IARC TP53 database’, *Hum. Mutat.*, vol. 28, no. 6, pp. 622–629, Jun. 2007, doi: 10.1002/humu.20495.

[69] X. Wang *et al.*, ‘The impact of hepatocyte nuclear factor-1α on liver malignancies and cell stemness with metabolic consequences’, *Stem Cell Res. Ther.*, vol. 10, no. 1, p. 315, Dec. 2019, doi: 10.1186/s13287-019-1438-z.

[70] Y. Miyachi, T. Miyazawa, and Y. Ogawa, ‘HNF1A Mutations and Beta Cell Dysfunction in Diabetes’, *Int. J. Mol. Sci.*, vol. 23, no. 6, p. 3222, Mar. 2022, doi: 10.3390/ijms23063222.

[71] J.-M. Servitja *et al.*, ‘Hnf1α (MODY3) Controls Tissue-Specific Transcriptional Programs and Exerts Opposed Effects on Cell Growth in Pancreatic Islets and Liver’, *Mol. Cell. Biol.*, vol. 29, no. 11, pp. 2945–2959, Jun. 2009, doi: 10.1128/MCB.01389-08.

[72] A. S. Teeli, K. Łuczyńska, E. Haque, M. A. Gayas, D. Winiarczyk, and H. Taniguchi, ‘Disruption of Tumor Suppressors HNF4α/HNF1α Causes Tumorigenesis in Liver’, *Cancers*, vol. 13, no. 21, p. 5357, Oct. 2021, doi: 10.3390/cancers13215357.

[73] T. Nammo *et al.*, ‘Expression profile of MODY3/HNF-1alpha protein in the developing mouse pancreas’, *Diabetologia*, vol. 45, no. 8, pp. 1142–1153, Aug. 2002, doi: 10.1007/s00125-002-0892-8.

[74] Y. Sato *et al.*, ‘HNF1α controls glucagon secretion in pancreatic α-cells through modulation of SGLT1’, *Biochim. Biophys. Acta BBA - Mol. Basis Dis.*, vol. 1866, no. 11, p. 165898, Nov. 2020, doi: 10.1016/j.bbadis.2020.165898.

[75] Y. H. Lee, B. Sauer, and F. J. Gonzalez, ‘Laron dwarfism and non-insulin-dependent diabetes mellitus in the Hnf-1alpha knockout mouse’, *Mol. Cell. Biol.*, vol. 18, no. 5, pp. 3059–3068, May 1998, doi: 10.1128/MCB.18.5.3059.

[76] M. A. Garcia-Gonzalez *et al.*, ‘A suppressor locus for MODY3-diabetes’, *Sci. Rep.*, vol. 6, p. 33087, Sep. 2016, doi: 10.1038/srep33087.

[77] J. Tan *et al.*, ‘HNF1 *α* Controls Liver Lipid Metabolism and Insulin Resistance via Negatively Regulating the SOCS-3-STAT3 Signaling Pathway’, *J. Diabetes Res.*, vol. 2019, pp. 1–15, May 2019, doi: 10.1155/2019/5483946.

[78] S. Althari *et al.*, ‘Unsupervised Clustering of Missense Variants in HNF1A Using Multidimensional Functional Data Aids Clinical Interpretation’, *Am. J. Hum. Genet.*, vol. 107, no. 4, pp. 670–682, Oct. 2020, doi: 10.1016/j.ajhg.2020.08.016.

[79] H. Wang, P. A. Antinozzi, K. A. Hagenfeldt, P. Maechler, and C. B. Wollheim, ‘Molecular targets of a human HNF1 alpha mutation responsible for pancreatic beta-cell

dysfunction', *EMBO J.*, vol. 19, no. 16, pp. 4257–4264, Aug. 2000, doi: 10.1093/emboj/19.16.4257.

[80] P. Maechler and C. B. Wollheim, 'Mitochondrial function in normal and diabetic beta-cells', *Nature*, vol. 414, no. 6865, pp. 807–812, Dec. 2001, doi: 10.1038/414807a.

[81] J.-C. Nault *et al.*, 'Molecular Classification of Hepatocellular Adenoma Associates With Risk Factors, Bleeding, and Malignant Transformation', *Gastroenterology*, vol. 152, no. 4, pp. 880-894.e6, Mar. 2017, doi: 10.1053/j.gastro.2016.11.042.

[82] Z. Luo *et al.*, 'Hepatocyte Nuclear Factor 1A (HNF1A) as a Possible Tumor Suppressor in Pancreatic Cancer', *PLOS ONE*, vol. 10, no. 3, p. e0121082, Mar. 2015, doi: 10.1371/journal.pone.0121082.

[83] L. Pelletier *et al.*, 'Loss of hepatocyte nuclear factor 1α function in human hepatocellular adenomas leads to aberrant activation of signaling pathways involved in tumorigenesis', *Hepatology*, vol. 51, no. 2, pp. 557–566, Feb. 2010, doi: 10.1002/hep.23362.

[84] K. Ozaki *et al.*, 'Hepatocyte nuclear factor 1α-inactivated hepatocellular adenomas exhibit high (18)F-fludeoxyglucose uptake associated with glucose-6-phosphate transporter inactivation', *Br. J. Radiol.*, vol. 89, no. 1063, p. 20160265, Jul. 2016, doi: 10.1259/bjr.20160265.

[85] H. Furuta *et al.*, 'Organization and partial sequence of the hepatocyte nuclear factor-4 alpha/MODY1 gene and identification of a missense mutation, R127W, in a Japanese family with MODY', *Diabetes*, vol. 46, no. 10, pp. 1652–1657, Oct. 1997, doi: 10.2337/diacare.46.10.1652.

[86] O. Bluteau *et al.*, 'Bi-allelic inactivation of TCF1 in hepatic adenomas', *Nat. Genet.*, vol. 32, no. 2, pp. 312–315, Oct. 2002, doi: 10.1038/ng1001.

[87] M. B. Raft, E. N. Jørgensen, and B. Vainer, 'Gene mutations in hepatocellular adenomas', *Histopathology*, vol. 66, no. 7, pp. 910–921, Jun. 2015, doi: 10.1111/his.12539.

[88] J.-C. Nault, P. Bioulac-Sage, and J. Zucman-Rossi, 'Hepatocellular benign tumors-from molecular classification to personalized clinical care', *Gastroenterology*, vol. 144, no. 5, pp. 888–902, May 2013, doi: 10.1053/j.gastro.2013.02.032.

[89] A. D. Tward *et al.*, 'Distinct pathways of genomic progression to benign and malignant tumors of the liver', *Proc. Natl. Acad. Sci. U. S. A.*, vol. 104, no. 37, pp. 14771–14776, Sep. 2007, doi: 10.1073/pnas.0706578104.

[90] J. F. Hechtman *et al.*, 'Somatic HNF1A mutations in the malignant transformation of hepatocellular adenomas: a retrospective analysis of data from MSK-IMPACT and TCGA', *Hum. Pathol.*, vol. 83, pp. 1–6, Jan. 2019, doi: 10.1016/j.humpath.2018.08.004.

[91] L. Pelletier, S. Rebouissou, D. Vignjevic, P. Bioulac-Sage, and J. Zucman-Rossi, 'HNF1α inhibition triggers epithelial-mesenchymal transition in human liver cancer cell lines', *BMC Cancer*, vol. 11, p. 427, Oct. 2011, doi: 10.1186/1471-2407-11-427.

[92] E. V. Abel *et al.*, 'HNF1A is a novel oncogene that regulates human pancreatic cancer stem cell properties', *eLife*, vol. 7, p. e33947, Aug. 2018, doi: 10.7554/eLife.33947.

[93] C. Patitucci *et al.*, 'Hepatocyte nuclear factor 1α suppresses steatosis-associated liver cancer by inhibiting PPARγ transcription', *J. Clin. Invest.*, vol. 127, no. 5, pp. 1873–1888, May 2017, doi: 10.1172/JCI90327.

[94] Z. Luo *et al.*, 'Hepatocyte nuclear factor 1A (HNF1A) as a possible tumor suppressor in pancreatic cancer', *PloS One*, vol. 10, no. 3, p. e0121082, 2015, doi: 10.1371/journal.pone.0121082.

[95] J. W. Hoskins *et al.*, 'Transcriptome analysis of pancreatic cancer reveals a tumor suppressor function for HNF1A', *Carcinogenesis*, vol. 35, no. 12, pp. 2670–2678, Dec. 2014, doi: 10.1093/carcin/bgu193.

[96] D. Q. Shih *et al.*, 'Loss of HNF-1alpha function in mice leads to abnormal expression of genes involved in pancreatic islet development and metabolism', *Diabetes*, vol. 50, no. 11, pp. 2472–2480, Nov. 2001, doi: 10.2337/diabetes.50.11.2472.

[97] F. Isidori *et al.*, 'Targeted Sequencing of Sorted Esophageal Adenocarcinoma Cells Unveils Known and Novel Mutations in the Separated Subpopulations', *Clin. Transl. Gastroenterol.*, vol. 11, no. 9, p. e00202, Sep. 2020, doi: 10.14309/ctg.0000000000000202.

[98] E. Bonora *et al.*, 'Biallelic variants in LIG3 cause a novel mitochondrial neurogastrointestinal encephalomyopathy', *Brain J. Neurol.*, vol. 144, no. 5, pp. 1451–1466, Jun. 2021, doi: 10.1093/brain/awab056.

[99] J. C. Rockett, K. Larkin, S. J. Darnton, A. G. Morris, and H. R. Matthews, 'Five newly established oesophageal carcinoma cell lines: Phenotypic and immunological characterization', *Br. J. Cancer*, vol. 75, no. 2, pp. 258–263, Jan. 1997, doi: 10.1038/bjc.1997.42.

[100] J. J. Boonstra *et al.*, 'Verification and unmasking of widely used human esophageal adenocarcinoma cell lines', *J. Natl. Cancer Inst.*, vol. 102, no. 4, pp. 271–274, Feb. 2010, doi: 10.1093/jnci/djp499.

[101] X. Rao, X. Huang, Z. Zhou, and X. Lin, 'An improvement of the 2ˆ(-delta delta CT) method for quantitative real-time polymerase chain reaction data analysis', *Biostat. Bioinforma. Biomath.*, vol. 3, no. 3, pp. 71–85, Aug. 2013.

[102] U. D. Kabra *et al.*, 'Direct Substrate Delivery Into Mitochondrial Fission-Deficient Pancreatic Islets Rescues Insulin Secretion', *Diabetes*, vol. 66, no. 5, pp. 1247–1257, May 2017, doi: 10.2337/db16-1088.

[103] K. A. Jagadeesh *et al.*, 'M-CAP eliminates a majority of variants of uncertain significance in clinical exomes at high sensitivity', *Nat. Genet.*, vol. 48, no. 12, pp. 1581–1586, Dec. 2016, doi: 10.1038/ng.3703.

[104] J. Marill, T. Cresteil, M. Lanotte, and G. G. Chabot, 'Identification of human cytochrome P450s involved in the formation of all-trans-retinoic acid principal metabolites', *Mol. Pharmacol.*, vol. 58, no. 6, pp. 1341–1348, Dec. 2000, doi: 10.1124/mol.58.6.1341.

[105] Z. Wu *et al.*, 'CYP2J2 and CYP2C19 are the major enzymes responsible for metabolism of albendazole and fenbendazole in human liver microsomes and recombinant P450 assay systems', *Antimicrob. Agents Chemother.*, vol. 57, no. 11, pp. 5448–5456, Nov.

2013, doi: 10.1128/AAC.00843-13.

[106] W. Abdelhamed and M. El-Kassas, 'Fibrolamellar hepatocellular carcinoma: A rare but unpleasant event', *World J. Gastrointest. Oncol.*, vol. 14, no. 6, pp. 1103–1114, Jun. 2022, doi: 10.4251/wjgo.v14.i6.1103.

[107] X. Jiang *et al.*, 'Targeting PI4KA sensitizes refractory leukemia to chemotherapy by modulating the ERK/AMPK/OXPHOS axis', *Theranostics*, vol. 12, no. 16, pp. 6972–6988, 2022, doi: 10.7150/thno.76563.

[108] M. Umair *et al.*, 'Exome sequencing revealed a splice site variant in the IQCE gene underlying post-axial polydactyly type A restricted to lower limb', *Eur. J. Hum. Genet.*, vol. 25, no. 8, pp. 960–965, Aug. 2017, doi: 10.1038/ejhg.2017.83.

[109] J. Yang *et al.*, 'Identification and characterization of novel fusion genes in prostate cancer by targeted RNA capture and next-generation sequencing', *Acta Biochim. Biophys. Sin.*, vol. 50, no. 11, pp. 1166–1172, Oct. 2018, doi: 10.1093/abbs/gmy112.

[110] S. C. Lim, J. Hroudová, N. J. Van Bergen, M. I. G. L. Sanchez, I. A. Trounce, and M. McKenzie, 'Loss of mitochondrial DNA-encoded protein ND1 results in disruption of complex I biogenesis during early stages of assembly', *FASEB J.*, vol. 30, no. 6, pp. 2236–2248, Jun. 2016, doi: 10.1096/fj.201500137R.

[111] Y.-Y. Bao, S.-H. Zhou, Z.-J. Lu, J. Fan, and Y.-P. Huang, 'Inhibiting GLUT-1 expression and PI3K/Akt signaling using apigenin improves the radiosensitivity of laryngeal carcinoma in vivo', *Oncol. Rep.*, vol. 34, no. 4, pp. 1805–1814, Oct. 2015, doi: 10.3892/or.2015.4158.

[112] H. Botha *et al.*, 'The Role of Glucose Transporters in Oral Squamous Cell Carcinoma', *Biomolecules*, vol. 11, no. 8, p. 1070, Jul. 2021, doi: 10.3390/biom11081070.

[113] O. Beylerli, G. Sufianova, A. Shumadalova, D. Zhang, and I. Gareev, 'MicroRNAs-mediated regulation of glucose transporter (GLUT) expression in glioblastoma', *Non-Coding RNA Res.*, vol. 7, no. 4, pp. 205–211, Dec. 2022, doi: 10.1016/j.ncrna.2022.09.001.

[114] R. L. Jones *et al.*, 'The prognostic significance of Ki67 before and after neoadjuvant chemotherapy in breast cancer', *Breast Cancer Res. Treat.*, vol. 116, no. 1, pp. 53–68, Jul. 2009, doi: 10.1007/s10549-008-0081-7.

[115] R. Burcombe *et al.*, 'Evaluation of Ki-67 proliferation and apoptotic index before, during and after neoadjuvant chemotherapy for primary breast cancer', *Breast Cancer Res.*, vol. 8, no. 3, p. R31, Jun. 2006, doi: 10.1186/bcr1508.

[116] E. Xu *et al.*, 'Genome-wide methylation analysis shows similar patterns in Barrett's esophagus and esophageal adenocarcinoma', *Carcinogenesis*, vol. 34, no. 12, pp. 2750–2756, Dec. 2013, doi: 10.1093/carcin/bgt286.

[117] H. Alvarez *et al.*, 'Widespread Hypomethylation Occurs Early and Synergizes with Gene Amplification during Esophageal Carcinogenesis', *PLoS Genet.*, vol. 7, no. 3, p. e1001356, Mar. 2011, doi: 10.1371/journal.pgen.1001356.

[118] L. B. Alexandrov, S. Nik-Zainal, D. C. Wedge, P. J. Campbell, and M. R. Stratton,

‘Deciphering signatures of mutational processes operative in human cancer’, *Cell Rep.*, vol. 3, no. 1, pp. 246–259, Jan. 2013, doi: 10.1016/j.celrep.2012.12.008.

[119] C. S. Ross-Innes *et al.*, ‘Whole-genome sequencing provides new insights into the clonal architecture of Barrett’s esophagus and esophageal adenocarcinoma’, *Nat. Genet.*, vol. 47, no. 9, pp. 1038–1046, Sep. 2015, doi: 10.1038/ng.3357.

[120] L. B. Alexandrov *et al.*, ‘The repertoire of mutational signatures in human cancer’, *Nature*, vol. 578, no. 7793, pp. 94–101, Feb. 2020, doi: 10.1038/s41586-020-1943-3.

[121] ICGC/TCGA Pan-Cancer Analysis of Whole Genomes Consortium, ‘Pan-cancer analysis of whole genomes’, *Nature*, vol. 578, no. 7793, pp. 82–93, Feb. 2020, doi: 10.1038/s41586-020-1969-6.

[122] A. M. Frankell *et al.*, ‘The landscape of selection in 551 esophageal adenocarcinomas defines genomic biomarkers for the clinic’, *Nat. Genet.*, vol. 51, no. 3, pp. 506–516, Mar. 2019, doi: 10.1038/s41588-018-0331-5.

[123] S. Nik-Zainal *et al.*, ‘Mutational processes molding the genomes of 21 breast cancers’, *Cell*, vol. 149, no. 5, pp. 979–993, May 2012, doi: 10.1016/j.cell.2012.04.024.

[124] K. Nones *et al.*, ‘Genomic catastrophes frequently arise in esophageal adenocarcinoma and drive tumorigenesis’, *Nat. Commun.*, vol. 5, p. 5224, Oct. 2014, doi: 10.1038/ncomms6224.

[125] EAC-BAGH group *et al.*, ‘Genomic profiles of primary and metastatic esophageal adenocarcinoma identified via digital sorting of pure cell populations: results from a case report’, *BMC Cancer*, vol. 18, no. 1, p. 889, Dec. 2018, doi: 10.1186/s12885-018-4789-4.

[126] C.-A. J. Ong, P. Lao-Sirieix, and R. C. Fitzgerald, ‘Biomarkers in Barrett’s esophagus and esophageal adenocarcinoma: predictors of progression and prognosis’, *World J. Gastroenterol.*, vol. 16, no. 45, pp. 5669–5681, Dec. 2010, doi: 10.3748/wjg.v16.i45.5669.

[127] F. M. Smith, R. B. Stephens, M. J. Kennedy, and J. V. Reynolds, ‘P53 abnormalities and outcomes in colorectal cancer: a systematic review’, *Br. J. Cancer*, vol. 92, no. 9, p. 1813, May 2005, doi: 10.1038/sj.bjc.6602589.

[128] M. Olivier *et al.*, ‘The clinical value of somatic TP53 gene mutations in 1,794 patients with breast cancer’, *Clin. Cancer Res. Off. J. Am. Assoc. Cancer Res.*, vol. 12, no. 4, pp. 1157–1167, Feb. 2006, doi: 10.1158/1078-0432.CCR-05-1029.

[129] M. F. Bellini, A. C. T. Cadamuro, M. Succi, M. A. Proença, and A. E. Silva, ‘Alterations of the TP53 gene in gastric and esophageal carcinogenesis’, *J. Biomed. Biotechnol.*, vol. 2012, p. 891961, 2012, doi: 10.1155/2012/891961.

[130] P. B. S. Lai, T.-Y. Chi, and G. G. Chen, ‘Different levels of p53 induced either apoptosis or cell cycle arrest in a doxycycline-regulated hepatocellular carcinoma cell line in vitro’, *Apoptosis Int. J. Program. Cell Death*, vol. 12, no. 2, pp. 387–393, Feb. 2007, doi: 10.1007/s10495-006-0571-1.

[131] C. R. Coffill *et al.*, ‘Mutant p53 interactome identifies nardilysin as a p53R273H-specific binding partner that promotes invasion’, *EMBO Rep.*, vol. 13, no. 7, pp. 638–644,

Jun. 2012, doi: 10.1038/embor.2012.74.

[132] K. Eguchi, T. Yao, T. Konomoto, K. Hayashi, M. Fujishima, and M. Tsuneyoshi, 'Discordance of p53 mutations of synchronous colorectal carcinomas', *Mod. Pathol. Off. J. U. S. Can. Acad. Pathol. Inc*, vol. 13, no. 2, pp. 131–139, Feb. 2000, doi: 10.1038/modpathol.3880024.

[133] N.-L. Sim, P. Kumar, J. Hu, S. Henikoff, G. Schneider, and P. C. Ng, 'SIFT web server: predicting effects of amino acid substitutions on proteins', *Nucleic Acids Res.*, vol. 40, no. Web Server issue, pp. W452-457, Jul. 2012, doi: 10.1093/nar/gks539.

[134] I. A. Adzhubei *et al.*, 'A method and server for predicting damaging missense mutations', *Nat. Methods*, vol. 7, no. 4, pp. 248–249, Apr. 2010, doi: 10.1038/nmeth0410-248.

[135] J. M. R. Lambert, A. Moshfegh, P. Hainaut, K. G. Wiman, and V. J. N. Bykov, 'Mutant p53 reactivation by PRIMA-1MET induces multiple signaling pathways converging on apoptosis', *Oncogene*, vol. 29, no. 9, pp. 1329–1338, Mar. 2010, doi: 10.1038/onc.2009.425.

[136] A. W. T. Ng *et al.*, 'Rearrangement processes and structural variations show evidence of selection in oesophageal adenocarcinomas', *Commun. Biol.*, vol. 5, no. 1, p. 335, Apr. 2022, doi: 10.1038/s42003-022-03238-7.

[137] H.-X. Wu *et al.*, 'Tumor mutational and indel burden: a systematic pan-cancer evaluation as prognostic biomarkers', *Ann. Transl. Med.*, vol. 7, no. 22, p. 640, Nov. 2019, doi: 10.21037/atm.2019.10.116.

[138] J. Ferlay *et al.*, 'Cancer incidence and mortality worldwide: sources, methods and major patterns in GLOBOCAN 2012', *Int. J. Cancer*, vol. 136, no. 5, pp. E359-386, Mar. 2015, doi: 10.1002/ijc.29210.

[139] I. Dagogo-Jack and A. T. Shaw, 'Tumour heterogeneity and resistance to cancer therapies', *Nat. Rev. Clin. Oncol.*, vol. 15, no. 2, pp. 81–94, Feb. 2018, doi: 10.1038/nrclinonc.2017.166.